Manuscript Details

Manuscript number	ENVPOL_2019_768
Title	ANOMALOUS CONCENTRATIONS OF ARSENIC, FLUORIDE AND RADON IN VOLCANIC-SEDIMENTARY AQUIFERS FROM CENTRAL ITALY: QUALITY INDEXES FOR MANAGEMENT OF THE WATER RESOURCE
Article type	Research Paper

Abstract

Six hundred and fifty-nine water samples from springs and wells in the Sabatini and the Vicano-Cimino Volcanic Districts (central Italy) were analyzed for arsenic (As), fluoride (F-) and radon (222Rn) concentrations. Waters mostly sourced from a shallow and cold aquifer hosted within volcanic rocks, which represents the main public drinking water supply. Cold waters from shallow perched aquifers within sedimentary formations and thermal waters related to a deep hydrothermal reservoir were also analyzed. The highest concentrations of As and F- were measured in the thermal waters and attributed to their enhanced mobility during water-rock interaction processes at hydrothermal temperature. Relatively high concentrations of As and F- were also recorded in those springs and wells discharging from the volcanic aquifer, whereas waters hosted in the sedimentary units showed significantly lower contents. About 60% (As) and 25% (F-) of cold waters from the volcanic aquifer exceeded the maximum allowable concentrations for human consumption. Such anomalously high levels of geogenic pollutants were caused by mixing with fluids upwelling through faulted zones from the hydrothermal reservoir. Chemical weathering of volcanic rocks and groundwater flow path were considered to contribute to a lesser extent to the observed As and F- concentrations. Cold waters from the volcanic aquifer showed the highest 222Rn concentrations, resulting from the high contents of Rn-generating radionuclides in the volcanic units. Approximately 22% of waters from the volcanic aquifer exceeded the recommended value for human consumption. The concentrations of the three parameters were used to determine a quality index (from the lowest, 1 to the highest, 4) for each water sample. Spatial distribution maps were then processed by means of geostatistical techniques. These maps represent a useful tool for water management by local authorities to both improve intervention plans in the contaminated sectors and identify new water resources suitable for human consumption.

Keywords	Arsenic; Fluoride; Radon; Central Italy; Geostatistical Techniques; Quality Index.

Corresponding Author	Daniele Cinti
Order of Authors	Daniele Cinti, Pier Paolo Poncia, Lorenzo Brusca, Fausto Grassa, Monia Procesi, Franco Tassi, Orlando Vaselli

Suggested reviewers	Brunella Raco, Dario TEDESCO, Thomas Darrah, Paul R.D. Mason, Dornadula Chandrasekharam

Submission Files Included in this PDF

File Name [File Type]

cover letter.docx [Cover Letter]

Research highlights.docx [Highlights]

graphical abstract.eps [Graphical Abstract]

manuscript 12february19_env pollut.docx [Manuscript File]

Figure_1.eps [Figure]

Figure_2.eps [Figure]

Figure_3.eps [Figure]

Figure_4.eps [Figure]

Figure_5.eps [Figure]

Figure_6.eps [Figure]

SM 2.eps [Figure]

SM 4.eps [Figure]

SM 5.eps [Figure]

SM 6.eps [Figure]

Table 1.docx [Table]

Table 2.docx [Table]

Table 3.docx [Table]

SM_1.docx [Table]

SM_3.docx [Table]

SM_7.docx [Table]

To view all the submission files, including those not included in the PDF, click on the manuscript title on your EVISE Homepage, then click 'Download zip file'.

INGV terremoti vulcani ambiente
ISTITUTO NAZIONALE DI GEOFISICA E VULCANOLOGIA

To the Editor of
Environmental Pollution

Dear Editor,

We are pleased to submit to Environmental Pollution the paper titled "*Anomalous concentrations of arsenic, fluoride and radon in volcanic-sedimentary aquifers from central Italy: quality indexes for management of the water resource*" by Daniele Cinti, Pier Paolo Poncia, Lorenzo Brusca, Fausto Grassa, Monia Procesi, Franco Tassi and Orlando Vaselli.

The manuscript is focused on the spatial distribution of three geogenic pollutants (arsenic, fluoride and radon) that seriously affect the groundwater systems hosted in two volcanic-sedimentary areas of central Italy. Water samples were collected from municipal and domestic wells and springs, most of which are used for human consumption, in the Sabatini and Vicano-Cimino volcanic districts (Latium region, Italy). Thermal waters fed by a deep-seated hydrothermal reservoir were also collected. A large chemical dataset is presented and concentration maps are drawn by means of geostatistical techniques (i.e. variogram models and kriging estimation). Additionally, a quality index was defined on the basis of the combined As, F^- and ^{222}Rn concentrations, and then mapped. The sources of geogenic pollutants and the main factors controlling their distribution in the different types of waters are discussed. Distribution maps were described as an essential source of information for the development of intervention plans aimed at discovering new water resources for human consumption and mitigating the impact of geogenic contamination on groundwater quality.

Hoping that you can consider our manuscript suitable to be peer-reviewed, we suggest names and e-mail addresses of five potential reviewers, as follows:

Dario Tedesco – Università della Campania	dario.tedesco@unicampania.it
Tom Darrah – Ohio State University	darrah.24@osu.edu
Paul Mason – Utrecht University	p.mason@uu.nl
Dornadula Chandrasekharam – Indian Institute of Technology	dchandra50@gmail.com
Brunella Raco – National Research Council (CNR)	brunella.raco@igg.cnr.it

Best Regards

Roma, February 15th, 2019

On the behalf of all the Authors
Daniele Cinti

Sezione RM1
Sismologia e Tettonofisica
Via di Vigna Murata, 605
00143 ROMA | Italia
Tel.: +39 06518601
Fax: +39 0651860507
aoo.roma1@pec.ingv.it
www.roma1.ingv.it

Should you need any further detail, please do not hesitate to contact me at the following coordinates:

Daniele Cinti: Tel. +39 06 51860 625
E-mail address: daniele.cinti@ingv.it

Research highlights

1) Water sampling was carried out in volcanic-sedimentary aquifers from Central Italy

2) Sources of geogenic pollutants (As, F^- and ^{222}Rn) were determined and discussed

3) Quality indexes were determined for waters by combining the As, F^- and ^{222}Rn contents

4) Geostatistical techniques were used to process distribution maps

5) Distribution maps as a tool for water management in geogenically polluted areas

sampling of waters in volcanic-sedimentary aquifers from Central Italy for As, F^- and ^{222}Rn concentrations

DISTRIBUTION MAPS AS A TOOL FOR WATER MANAGEMENT IN GEOGENICALLY POLLUTED AREAS

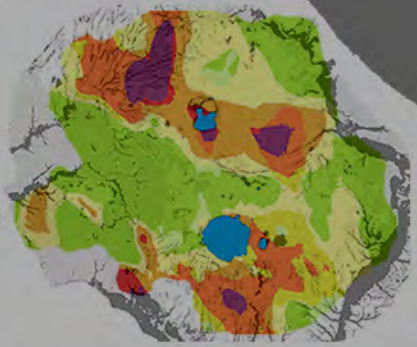

by combining the concentrations of As, F^- and ^{222}Rn a quality index is determined for each water sample and the relative distribution map is processed

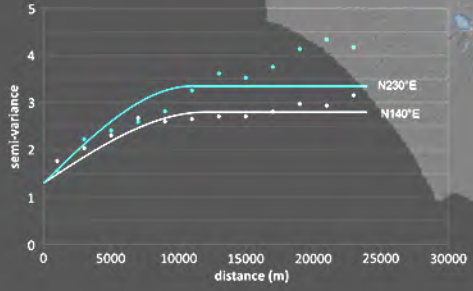

geostatistical techniques are used to process distribution maps

ANOMALOUS CONCENTRATIONS OF ARSENIC, FLUORIDE AND RADON IN VOLCANIC-SEDIMENTARY AQUIFERS FROM CENTRAL ITALY: QUALITY INDEXES FOR MANAGEMENT OF THE WATER RESOURCE

Cinti, D. (1), Poncia, P.P. (2), Brusca, L. (3), Grassa, F. (3), Procesi, M. (1), Tassi, F. (4,5), Vaselli, O. (4,5)*

(1) Istituto Nazionale di Geofisica e Vulcanologia, Via di Vigna Murata, 605 - 00143 Roma, Italy

(2) via Camerano 1, 01028 Orte, Italy

(3) Istituto Nazionale di Geofisica e Vulcanologia, Via U. La Malfa, 153 - 90146 Palermo, Italy

(4) Dipartimento di Scienze della Terra, Università di Firenze, via G. La Pira 4, 50121 Firenze, Italy

(5) CNR - Istituto di Geoscienze e Scienze della Terra, via G. La Pira 4, 50121 Firenze, Italy

**Corresponding author, E–mail: daniele.cinti@ingv.it*

Abstract

Six hundred and fifty-nine water samples from springs and wells in the Sabatini and the Vicano-Cimino Volcanic Districts (central Italy) were analyzed for arsenic (As), fluoride (F^-) and radon (^{222}Rn) concentrations. Waters mostly sourced from a shallow and cold aquifer hosted within volcanic rocks, which represents the main public drinking water supply. Cold waters from shallow perched aquifers within sedimentary formations and thermal waters related to a deep hydrothermal reservoir were also analyzed. The highest concentrations of As and F^- were measured in the thermal waters and attributed to their enhanced mobility during water-rock interaction processes at hydrothermal temperature. Relatively high concentrations of As and F^- were also recorded in those springs and wells discharging from the volcanic aquifer, whereas waters hosted in the sedimentary units showed significantly lower contents. About 60% (As) and 25% (F^-) of cold waters from the volcanic aquifer exceeded the maximum allowable concentrations for human consumption. Such

anomalously high levels of geogenic pollutants were caused by mixing with fluids upwelling through faulted zones from the hydrothermal reservoir. Chemical weathering of volcanic rocks and groundwater flow path were considered to contribute to a lesser extent to the observed As and F^- concentrations. Cold waters from the volcanic aquifer showed the highest ^{222}Rn concentrations, resulting from the high contents of Rn-generating radionuclides in the volcanic units. Approximately 22% of waters from the volcanic aquifer exceeded the recommended value for human consumption. The concentrations of the three parameters were used to determine a quality index (from the lowest, 1 to the highest, 4) for each water sample. Spatial distribution maps were then processed by means of geostatistical techniques. These maps represent a useful tool for water management by local authorities to both improve intervention plans in the contaminated sectors and identify new water resources suitable for human consumption.

Keywords

Arsenic; Fluoride; Radon; Central Italy; Geostatistical Techniques; Quality Index

1. Introduction

The peri-Tyrrhenian sector of central Italy, from southern Tuscany to northern Latium, hosts large (>1000 km^2 wide) Quaternary potassic and ultrapotassic volcanic districts (Vulsini, Vicano-Cimino, Sabatini and Colli Albani; Conticelli and Peccerillo, 1992). These systems are currently considered in a dormant stage, since the last eruptive event dated back 36 ka (Marra et al., 2009). As a result, volcanic hazard in these areas does not include any potentially dangerous eruptive phenomena and secondary eruption-related processes (e.g. volcanic earthquakes, lahars or tsunamis), but medium- to long-term phenomena still active since the end of the volcanic activity. Among them, local uprising of deep-originated hydrothermal fluids and their interaction with volcanic rocks are able to cause groundwater pollution with the consequent deterioration of the quality of water resources for human consumption, as largely documented on active or dormant

53 volcanoes worldwide (e.g. Ellis and Mahon, 1977; Barnes, 1997; Aiuppa et al., 2000, 2005;
54 Dall'Aglio et al., 2001; Vivona et al., 2007).

55 In an effort to provide an adequate supply of safe water for household consumption, the
56 geochemical characterization of groundwater resources in volcanic-hydrothermal areas represents
57 an essential step to define the necessary tools for decision-making in territory planning. In this
58 respect, the present study focuses on the Sabatini Volcanic District (SVD) and the Vicano-Cimino
59 Volcanic District (VCVD), two wide (~2800 km^2) and densely populated areas (~500,000
60 inhabitants) in the Latium region, where the regional groundwater circulation within volcanic rocks
61 is the main source of cold and fresh waters used as drinking water supply. Recent studies
62 highlighted that groundwater quality can be compromised due to natural processes such as: *i*) excess
63 of solutes, which play an essential role for the human health status but only in a specific
64 concentration range (e.g. fluoride; Vivona et al., 2007; Preziosi et al., 2016), *ii*) occurrence of toxic
65 contaminants (e.g. arsenic and heavy metals; Angelone et al., 2009; Baiocchi et al., 2013; Armiento
66 et al., 2015; Cinti et al., 2015; Viaroli et al., 2016), and *iii*) anomalous concentrations of radioactive
67 isotopes (e.g. radon; Cinti et al., 2013). These contaminants can be responsible of harmful effects on
68 the environment and, particularly, on human health.

69 In this paper, we report the results related to the As, F^- and ^{222}Rn concentrations determined on
70 659 water samples, including thermal and cold springs, private domestic and municipal wells, from
71 SVD and VCVD. The main goals are to *i*) investigate the sources of these elements and the main
72 factors controlling their geochemical behaviour and *ii*) define their spatial distribution to evaluate
73 the potential health risk in the study area. In the framework of the model of the *Water Safety Plans*
74 (WHO, 2011) aimed at ensuring rigorous control strategies on water quality for health protection,
75 we defined a quality index (QI: from 1 to 4) for each water sample to establish the degree of natural
76 contamination of the water resource and provide a valid tool for water management by policy
77 makers.

78

2. Origin and behaviour of arsenic, fluoride and radon in natural waters

2.1. Arsenic

Arsenic (As) is a toxic element ubiquitously found in the environment (Nordstrom, 2002; Smedley and Kinniburgh, 2002; WHO, 2011) and classified as a carcinogenic (IARC, 2004). Acute and chronic toxic effects on populations exposed to high As concentrations in drinking water (WHO, 2011) promoted the legislative revision concerning the quality standards for drinking waters (Council Directive 98/83/EC), which lowered the As concentration limit from 50 to 10 μg/L and imposed a drastic change in the management of groundwater resources. Volcanic and hydrothermal environments are considered one of the main natural sources of As in groundwater. The occurrence of As in groundwater circulating in volcanic systems is related to the presence of this element as a minor constituent of volcanic gases and geothermal fluids due to the leaching of As-bearing minerals (e.g. sulfides, oxides, arsenates, arsenites) in volcanic rocks (Ballantyne and Moore, 1988; Smedley and Kinniburgh, 2002; Webster and Nordstrom, 2003; Aiuppa et al., 2006). Natural As contamination of drinking waters has widely been documented to occur worldwide (e.g. Smedley and Kinniburgh, 2002; Guo and Wang, 2005; Rahman et al., 2005; Bundschuh et al., 2009) including Italy (e.g. Aiuppa et al., 2003; Angelone et al., 2009; Baiocchi et al., 2013; Armiento et al., 2015; Cinti et al., 2015). Up to 150 million people are thought to be exposed to anomalous concentrations of As, although this evaluation is likely underestimated since new contaminated areas are continuously discovered (Ravenscroft et al., 2009). In aqueous solutions, As mostly occurs in inorganic forms, as oxyanions of arsenite As(III) or arsenate As(V) (WHO, 2011), and is easily mobilized at pH between 6.5 to 8.5 as typically shown by groundwater. Although As(V) is favored in oxidized environments and As(III) at anaerobic conditions, they are reported to coexist (Smedley and Kinniburgh, 2002; Oremland and Stolz, 2003). The As(III) compounds are considered to be more toxic and more difficult to be removed than those of As(V) (Bissen and Frimmel, 2003).

2.2. Fluoride

Fluorine is the 13th most abundant element in the Earth's crust (Weinstein and Davison, 2003), and its major pathway to humans is through drinking water as fluoride (F^-). Its optimal range for human health status is considered to be between 0.5 and 1.5 mg/L, a concentration range that is beneficial to prevent dental caries and strengthen bones (Fabiani et al., 1999; WHO, 2011). The artificial fluoridation of public supplied waters is a practice used in many countries of the world for waters having F^- concentration below <0.5 mg/L. On the other hand, chronic ingestion at high doses (>1.5 mg/L) of F^- can lead to adverse effects, including dental and skeletal fluorosis, whose severity is roughly proportional to its concentration in water (Edmunds and Smedley, 1996; Ozsvath, 2009). Endemic fluorosis is a major concern in many regions worldwide (e.g. Ren and Shugin, 1988; Choubisa, 1999; Reimann et al., 2003; Soto-Rojas et al., 2004), whereas in Italy fluorosis is limited to a few areas in Sicily (Fradà et al., 1969). High F^- concentrations in groundwater are generally related to natural sources, though occasionally is of anthropogenic origin (Ozsvath, 2009; WHO, 2011). The occurrence of F^- in volcanic-hydrothermal fluids is related to *i*) release of magmatic fluorine as HF through volcanic degassing, *ii*) upwelling of geothermal fluids and *iii*) water-rock interaction processes involving F-rich minerals (e.g., D'Alessandro, 2006; Sawyer and Opperheimer, 2006; Ozsvath, 2009; De Rita et al., 2011). High fluorine contents are generally found in volcanic rocks and hydrothermal deposits commonly associated with fluorite (CaF_2), fluorapatite ($Ca_5(PO_4)_3F$) and F-rich micas and/or amphiboles (where F^- largely replaces OH^- within the mineral structures). Dissolved F^- concentrations are usually controlled by water temperature, pH, presence of complexing/precipitating ions and colloids, solubility of F-bearing minerals, residence time, and climate (Ozsvath, 2009). Accordingly, waters characterized by high temperatures and acidic conditions favor the presence of dissolved fluoride in volcanic aquifers.

2.3. Radon

Natural radionuclides, continuously produced in the Earth's crust by ^{238}U, ^{235}U and ^{232}Th radioactive chains and ^{40}K, that is a long-lived radioactive isotope of elemental K, represent the

main natural source of ionizing radiation received by the human population worldwide (UNSCEAR, 2008). Among them, radon-222 (^{222}Rn), formed within the ^{238}U chain by decay of ^{226}Ra, is the main radioactivity source of groundwater. Radon has three radioactive isotopes but only ^{222}Rn is of interest having a half-life of 3.8 days, since ^{219}Rn and ^{220}Rn are short-lived isotopes (3.8 sec and 55.6 sec, respectively). The health hazard associated with elevated concentrations of ^{222}Rn in drinking water mostly arises from inhalation of radon discharged from tap water in indoor air and, to a lesser extent, from direct ingestion. Radon is classified as a human carcinogen, whose long-term exposure via inhalation represents the second cause of lung cancer after smoking (Dubois, 2005). There is also evidence that prolonged ingestion of ^{222}Rn-rich water can cause stomach cancer (UNSCEAR, 2008; WHO, 2011). Following the EU guidelines on radioactive substances in water intended for human consumption (Council Directive 2013/51/EURATOM), Italy has recently set the concentration limit for ^{222}Rn in drinking water at 100 Bq/L (DLgs n° 28/2016), which represents the action level (Synnott and Fenton, 2005) above which an intervention is recommended to improve the quality of water to comply with the requirements for the protection of human health. An additional reference level of 1,000 Bq/L, i.e. ^{222}Rn concentration above which some specific decision should be taken, has also been defined. The occurrence of U- and Ra-rich rocks is the main factor determining high ^{222}Rn concentrations in groundwater (e.g. Loomis et al., 1988; Ball et al., 1991; Vinson et al., 2009; Cinti et al., 2013; Alonso et al., 2015). However, ^{222}Rn concentration in drinking water is strongly influenced by other factors such as the water distribution system and water purification operations, whereas the contribution of dissolved ^{222}Rn to the total indoor-airborne concentration inside the dwelling is influenced by the amount of water used, volume of the dwelling and ventilation rate (Hopke et al., 2000; UNSCEAR, 2008).

3. Geological, structural and hydrological settings

The study area includes VCVD and SVD, two of the four large (more than 1,000 km^2 each) Quaternary volcanic districts that constitute the Roman Magmatic Province (Conticelli and

Peccerillo, 1992), and the adjacent Tolfa mountains, which formed from the emplacement of an intrusive body pertaining to the Tuscan Magmatic Province (i.e. the Tolfa Dome Complex; Cimarelli and De Rita, 2006) on a sedimentary basement (Fig. 1). Magmatism in the Tyrrhenian sector of central Italy generated as the result of a post-collisional crustal extension that occurred at the back of the eastward-migrating Apennine fold-and-thrust belt. This extensional system also led to the development of dominant NW- and minor NE-striking extensional fault sets arranged in a horst-graben pattern (Barberi et al., 1994; Acocella and Funiciello, 2006), and produced a strong crustal thinning (<25 km; Scrocca et al., 2003) and high heat flow (locally >200 mW/m^2; Della Vedova et al., 2001). Volcanic complexes gdeveloped on buried horst-graben structures, as shown by gravimetric anomalies (Barberi et al., 1994), whilst marine clastic sediments filled the structural lows.

The volcanic activity took place in different phases separated in space and time, becoming progressively younger from east to west (Serri et al., 1993), and associated with important changes in the nature of the erupted magmas. It was initially characterized by crustal metasomatized acidic magmas pertaining to the Tuscan Magmatic Province, later evolving towards under-saturated alkali-potassic products of the Roman Magmatic Province (Peccerillo, 2017). In the study area, the acid products consist of rhyolites, rhyodacites and trachydacites mostly found as dome complexes, corresponding to the Tolfa-Cerite-Manziate (3.5 Ma) and the Cimini (1.3-0.9 Ma) domes (Cimarelli and De Rita, 2006; Peccerillo, 2017) (Fig. 1). Alkali-potassic Roman volcanics, consisting of potassic (thachybasalts, trachytes) and ultrapotassic (leucites, tephrites, phonolites) pyroclastics, phreatomagmatic deposits and minor lavas, generated a large volcanic complex (the Sabatini complex 0.8-0.09 Ma; Cioni et al., 1993; De Rita et al., 1996) and a stratovolcano (the Vicano complex 0.4-0.1 Ma; Laurenzi and Villa, 1987). The pre-volcanic basement of SVD and VCVD includes, from bottom to top (Fig. 1): *i*) Mesozoic carbonates overlying Triassic evaporitic facies (Burano Fm.) *ii*) a Cretaceous-Paleogene arenaceous-clayey-carbonate allochthonous flyschoid complex (Ligurian s.l.), and *iii*) a Miocene-Plio-Pleistocene autochthonous complex consisting of

183 continental marls, sands, clays, and conglomerates. The youngest formations are Quaternary
184 continental clastic sediments associated with travertines and diatomites (Baldi et al., 1974; Barberi
185 et al., 1994).

186 Two main aquifers at different depths can be distinguished in the study area: *i*) a shallow
187 volcanic aquifer, recharged by meteoric infiltration, and *ii*) a deep regional hydrothermal reservoir
188 confined within the carbonate-evaporite units and separated from the volcanic aquifer by the low-
189 permeability Plio–Pleistocene deposits and/or the Ligurian s.l. rocks (Capelli et al., 2005; Manca et
190 al., 2017). Locally, permeable layers within the low-permeability sedimentary deposits host perched
191 aquifers that feed numerous springs of limited and discontinuous extent. The volcanic aquifer is
192 made up of both fractured (lava flows) and porous (pyroclastic units) layers, the latter showing
193 marked lateral and vertical heterogeneities according to the depositional environment. Although
194 volcanic units are inhomogeneous in terms of geometry and hydraulic properties, at regional scale
195 all the volcanic layers can be regarded as large continuous multi-layered aquifer, sustained by the
196 less permeable pre-volcanic deposits (Manca et al., 2017). Thermal and mineral springs abundantly
197 emerge from the volcanic and sedimentary outcrops (Fig. 1) especially in correspondence of
198 tectonic disturbances, since fractures and faults act as preferential paths for upwelling deep-
199 originated fluids. By a hydrogeological point of view, groundwater circulation mainly reflects the
200 volcanic structures since radially flowing waters from the higher sectors of each volcanic district
201 were observed (Capelli et al., 2005). The volcanic aquifer mainly discharges from both linear
202 springs, continuously supplying watercourses of limited length but characterized by constant flow,
203 and punctual springs. Lakes Vico, Bracciano and Martignano represent the level of the volcanic
204 aquifer, whereas Lake Monterosi is related to a perched aquifer (Capelli et al., 2005; Baiocchi et al.,
205 2006; Manca et al., 2017).

206

207 **4. Methods**

208 *4.1 Sampling and analytical methods*

Water samples (N=259) were collected from springs, domestic and municipal wells over an area of approximately 2,800 km^2. The sampling sites were homogeneously distributed all over the investigated area with a relatively high sampling density (Fig. 1). Waters discharges are associated with *i*) the cold and shallow aquifer hosted in the volcanic rocks, *ii*) the cold and shallow perched aquifers hosted in the permeable layers of the low-permeability sedimentary deposits and *iii*) the deep hydrothermal reservoir hosted in the carbonate-evaporite formations. Many springs and wells from the volcanic aquifer supply the local drinking water. The main physical, chemical and isotopic features of the collected waters were reported elsewhere (Cinti et al., 2011, 2014, 2017).

Samples for the analysis of As were collected in polyethylene tubes, which were pre-cleaned in the laboratory with diluted (1:3) Suprapur HNO_3 and then thoroughly rinsed with ultra-pure deionized water. Each sample was filtered using 0.45 μm filters and then acidified to pH<2 with ultra-pure HNO_3 to avoid metal precipitation and/or metal adsorption on the tube surface. Elemental analyses were performed at the Trace Elements Laboratory of INGV in Palermo (Italy) by inductively coupled plasma mass spectrometer (ICP-MS Agilent 7500ce) equipped with a Micromist nebulizer, a Scott double pass spray chamber, a three-channel peristaltic pump and an Octolpole Reaction System for removing interferences of polyatomic masses in Helium-mode. Fluoride was analyzed on filtered (0.45 μm) samples by ion-chromatography (Dionex DX-500 and Thermo Scientific Dionex ICS-900) equipped with suppressor and conductivity detector. Analyses were performed at the Laboratory of Fluid Geochemistry of INGV in Rome (Italy). Samples for dissolved ^{222}Rn analyses were collected in a 0.6 L bottle equipped with a watertight cap provided with an expansion chamber, in order to allow an air bubble inside the bottle, and inserted in a closed circuit with a pump and an Activated Charcoal Collector (Mancini et al., 2000). The ^{222}Rn-enriched air was pumped from the expansion chamber of the bottle and pushes it toward the surface of the collector. Radon-222 stripped from water was then adsorbed into the activated charcoal. Collectors were analyzed at the Laboratory of Radionuclides of INGV in Rome (Italy) by a low background γ-spectrometer using a NaI(Tl) scintillator. The ^{222}Rn concentration was obtained by detecting the γ

radiation deriving from the radon decay products ^{214}Pb and ^{214}Bi and correcting the gross datum by a decay factor that accounted for radon decay from the sampling time to the analyzing time (Mancini et al., 2000).

4.2 Statistical and geostatistical analysis

Descriptive statistics and graphical representations were carried out to characterize the whole population of water samples and related subsets with respect to the geochemical parameters (As, F^- and ^{222}Rn concentrations). After the statistical analysis, the geochemical data were processed to produce contour maps by applying geostatistics techniques (i.e. variogram analysis and kriging estimation; Krige, 1966; Matheron, 1971; Goovaerts, 1997). Experimental directional variograms provided a description of the scale and pattern of spatial variation and the spatial model needed for kriging. In more details, they were constructed to *i*) investigate the spatial dependence of the As, F^- and ^{222}Rn concentrations by calculating the variogram parameters (nugget, range and sill), *ii*) determine the directional differences (anisotropy) for the kriging estimation (directions and ratio between the major and minor anisotropy ellipse axes), *iii*) model the experimental variograms by means of the geological information, *iv*) validate the selected model (cross-validation) for computing errors, thereby defining how well the model fits and *v*) estimate the spatial distribution of the studied variables using variogram model parameters in the kriging algorithm to construct contour maps. Kriging was applied to find the best local estimate of the mean value of a regionalized variable, i.e. a property that varies in the geographic space, by using the measured values and a semi-variogram to determine the scale of variance and estimate unknown values.

5. Results

5.1 Basic statistics

Arsenic, F^- and ^{222}Rn concentrations, geographical coordinates of the sampling sites, emergence and aquifer type and a map reporting the labelled sampling points are provided as electronic

supplementary material (SM 1 and SM 2, respectively). Basic statistics (Tab. 1) show that the experimental data are positively skewed (i.e. the average is higher than the median value) for the three elements and hereafter characterized by non-normal distribution. Arsenic concentrations range from 0.01 to 1514 μg/L with a median value of 10.6 μg/L and an Inter-Quartile Range (IQR=3rd quartile – 1st quartile; i.e. a measure of the statistical dispersion) of 19.5 μg/L. Fluoride concentrations were comprised between 0.01 and 16.5 mg/L with median and IQR values of 0.68 and 1.34 mg/L, respectively. Dissolved ^{222}Rn contents varied from 0.10 to 797 Bq/L (median and IQR values of 36.9 and 65.4 Bq/L, respectively).

Three different subsets were extracted from the whole dataset, as follows: *i*) cold waters from the volcanic aquifer, *ii*) cold waters from the shallow perched sedimentary aquifers and *iii*) thermal waters from the deep hydrothermal reservoir (Tab. 1). Cold waters circulating within the volcanic and sedimentary formations were firstly recognized on the basis of the outcropping unit at the sampling site (Fig. 1) and, where available, the well stratigraphy. Where such a criterion proved to be uncertain, e.g. at the border between volcanic and sedimentary formations, waters from the two groups were distinguished according to their chemical-physical features at the sampling site (e.g., Cinti et al., 2011). Experimental data relative to the three subsets (Tab. 1) show a positive skewness for each variable, except for the subset representing the F^- concentrations in thermal waters, which shows a normal distribution (i.e. the average is close to the median value). Box-plots (Fig. 2a-c) indicate that thermal waters were showing the highest concentrations and the largest dispersions for As and F^-, with median values of 77.3 μg/L and 2.15 mg/L and IQR values of 321 μg/L and 1.34 mg/L, respectively (Tab. 1). Cold waters from the volcanic aquifer displayed concentrations and dispersions (median values of 13.2 μg/L, 0.72 mg/L and 54.0 Bq/L and IQR values of 18.3 μg/L, 1.21 mg/L and 63.4 Bq/L for As, F^- and ^{222}Rn, respectively) relatively higher than those recorded for the sedimentary waters, which were characterized by the lowest concentrations and dispersions

for the three variables (median values of 1.06 μg/L, 0.23 mg/L and 6.37 Bq/L and IQR values of 3.93 μg/L, 0.44 mg/L and 8.91 Bq/L for As, F^- and ^{222}Rn, respectively; Fig. 2a-d).

5.2 Geostatistical analysis and kriging

A comprehensive geostatistical approach was elaborated in order to provide insights into the spatial distribution of As, F^- and ^{222}Rn and to construct distribution maps by means of ordinary kriging. Since the concentrations of As, F^- and ^{222}Rn exhibit non-normal distributions, i.e. the assumption of statistical normality is not initially satisfied, a log-transformation of the variables was applied to obtain a data distribution as close as possible to a Gaussian-type and to calculate more regular, i.e. easily interpretable, variograms during the structural analysis. In this respect, QQ-plots were drawn for a qualitative evaluation of the "normality" of the transformed variables. The comparison between the original and the transformed variables (see SM 3) shows that the latter approach produces a symmetrical distribution, although they cannot utterly be considered as Gaussian distributions, especially the logAs and $logF^-$ of thermal waters.

For each transformed variable, directional semi-variograms were computed for the estimation of the spatial variation of values of the regionalized variables (SM 4-6). Lag distances of 2,500 m for F^- and ^{222}Rn and 2000 m for As were used for computation, on the basis of the average minimum distance among pairs of samples. This representation considers the anisotropy of the variables and allows to validate the presence of spatial autocorrelation among the experimental data. The common features of the directional semi-variograms are, as follows: *i*) roughly linear growth of the semi-variance $\gamma(h)$ up to a certain lag distance (range) over which the semi-variance $\gamma(h)$ remains approximatively constant at a specific value (sill), which means that only sample locations separated by distances closer the range are spatially correlated, and *ii*) nugget effect, i.e. for lag=0 the semi-variance $\gamma(h)>0$, due to the measurement errors and/or spatial variations occurring at distances smaller than the sampling step. The geometric anisotropy for As is defined along the N140°E and N230°E directions (SM 4), as representative of major (u direction) and minor (v

311 direction) axes of anisotropy ellipse, respectively. The major axis (i.e. the direction of maximum
312 spatial continuity of the variable) is at the range of 12,000 m, whereas the minor axis (i.e. the
313 direction of maximum spatial variability of the variable) is at the range of 11,000 m. As regards to
314 F^-, the main directions of the geometric anisotropy are N160°E and N250°E for maximum
315 continuity (range of 9,000 m) and maximum variability (range of 8,500 m), respectively (SM 5).
316 The geometric anisotropy for ^{222}Rn is recognized along the N170°E and N260°E directions, for u
317 (range of 8,500 m) and v (range of 8,000 m) directions, respectively (SM 6). Model parameters and
318 cross-validation results were checked for the three elements and reported as supplementary material
319 (SM 7). Ordinary kriging was applied to produce estimation maps for log variables by using the
320 model parameters of SM 7. At a preliminary phase, maps were back-transformed into original
321 variable values and no further adjustments (e.g. removal of outliers) were carried out on maps after
322 kriging process.
323
324 **6. Discussion**
325 *6.1 Arsenic*
326 As shown by the contour map of Fig. 3, two main sectors characterized by severe As
327 contamination of waters were recognized *i*) along a NW-SE-oriented belt roughly extending from
328 Tuscania to Nepi and *ii*) to the south and east of the Bracciano lake. They correspond to areas of
329 intense discharge of fluids from the underlying hydrothermal reservoir, whose high temperatures
330 and abundance of acidic gas species (CO_2, H_2S) favor intense leaching of rocks and mobilization of
331 As during water-rock interaction processes (Ballantyne and Moore, 1988; Webster and Nordstrom,
332 2003; Aiuppa et al., 2006). This evidence coupled with the strong correlation of As with
333 temperature (Fig. 2a) suggest that the contamination of water resources from the volcanic aquifer is
334 strictly related with the hydrothermal processes. The fluids from the hydrothermal reservoir mostly
335 discharge along extensional faults and fractured zones bordering the buried structural highs of
336 the carbonate basement. This structural control, which was already hypothesized by previous

337 investigations (e.g., Chiodini et al., 1999; Minissale, 2004; Cinti et al., 2011, 2014), provides
338 permeable pathways for the deep-sourced ascending fluids. On the other hand, where the
339 volcanic aquifer shows no relation with the tectonic framework and the high thickness of low-
340 permeability sedimentary rocks hinders mixing between shallow and deep fluids, significantly
341 lower As concentration were found. This is particularly evident *i*) in the north-eastern sector of
342 the VCVD from the Cimini mountains to Orte and *ii*) in the large E-W-trending belt roughly
343 extending from Fiano to Manziana (Fig. 3). Here, when no mixing processes involving shallow
344 and deep fluids occur, As concentrations in groundwater are mainly controlled by *i*) the
345 lithology of the rock hosting the aquifer and *ii*) the groundwater flow path. The noticeably low
346 As concentrations (<5 μg/L) of the waters circulating within the perched aquifers are likely
347 due to the paucity of As in the sedimentary formations (Smedley and Kinniburgh, 2002). On the
348 other hand, volcanic rocks from the Roman Magmatic Province showed significantly higher As
349 contents (up to 42 and 187 mg/kg for lavas and pyroclastic deposits, respectively; Vivona et al.,
350 2007; Armiento et al., 2015; Piscopo et al., 2018) relative to those reported for other Italian
351 volcanic rocks (generally ranging from 1 to 12 mg/kg; Allard et al., 2000; Paone et al., 2001;
352 Aiuppa et al., 2003). Nevertheless, in the absence of a thermal and/or acidic input from depth,
353 weathering and dissolution of volcanic rocks seem to contribute only partially to the release of
354 As into the groundwater system, as suggested by leaching tests conducted on lavas and
355 pyroclastic deposits from the VCVD (Armiento et al., 2015). Therefore, the variable but
356 generally low (<20 μg/L) As concentrations in the volcanic aquifer are likely resulting from both
357 the different content of As in the lava and pyroclastic units and related to different hydrogeological
358 properties (i.e. fractured vs. porous media) controlling the circulation paths. Interestingly, where
359 the groundwater flow path is strongly influenced by human activities, e.g. where the over-
360 exploitation of wells induces a steeper vertical gradient, the lateral inflow of As-rich waters may
361 affect uncontaminated sectors (Baiocchi et al., 2013).

362

363 *6.2 Fluoride*

364 The spatial distribution of F^- concentrations (Fig. 4) is partially consistent with that of As, likely
365 due to *i*) the similar geochemical behavior of the two elements and *ii*) their preferential enrichment
366 in thermal waters than in cold waters (Fig. 2a-c). Waters with F^- concentrations >1.5 mg/L, i.e.
367 higher than the concentration limit for drinkable waters, discharge in correspondence with F-rich
368 deposits and hydrothermally altered volcanic rocks and recently formed travertines, the latter
369 largely occurring in SVD and VCVD (De Rita et al., 2011). F-rich waters are thus produced by
370 water-rock interaction processes involving such deposits, this process being also favored by
371 thermalism and deep-sourced CO_2 dissolution in the shallow aquifers (Chiodini et al., 1999;
372 Minissale, 2004). Similar to what observed for As, the uprising of thermal waters along regional
373 and/or local fractures is responsible for the F^- contamination of shallow water resources.
374 Conversely, F^- mobility is significantly limited in the absence of active hydrothermal and alteration
375 processes, as highlighted by results of leaching tests on volcanic rocks of SVD and VCVD (De Rita
376 et al., 2011). Accordingly, waters circulating within the sedimentary environment, where the
377 background values of F^- were estimated to be lower than those related to the volcanic rocks (in the
378 range 100-300 mg/kg and 600 mg/kg, respectively; Ellis and Mahon, 1977; Faure, 1991) show F^-
379 contents even lower than the threshold value of 0.5 mg/L.

380

381 *6.3 Radon*

382 The contour map of ^{222}Rn in groundwater (Fig. 5) is significantly different with respect to those
383 of As and F^-. It shows a preferential ^{222}Rn enrichment in the cold waters circulating within the
384 volcanic rock aquifers, thus suggesting that the aquifer lithology is the main factor controlling the
385 ^{222}Rn distribution in the study area (Fig. 2d). This is confirmed by the mean contents of Rn-
386 generating radionuclides ^{238}U and ^{226}Ra of tuffs (160 and 147 Bq/kg, respectively) and lavas (134
387 and 124 Bq/kg, respectively) from the Roman Magmatic Province, which were significantly higher

than those of sedimentary formations (up to 49 and 24 Bq/kg, respectively) (Locardi and Mittempergher, 1971; Voltaggio et al., 2001; Trevisi et al., 2005). Significant variations in the distribution map were also highlighted between the innermost areas, including the Cimini Dome and the Vico and Bracciano depressions, where ^{222}Rn contents were often >100 Bq/L (i.e. higher than the parametric recommended value for drinking waters), and the peripheral areas, where concentrations were generally lower (20-60 Bq/L). If it is assumed that the mean distribution of ^{222}Rn progenitors in the volcanic rocks is quite homogeneous, as evidenced by the similar concentrations of ^{238}U and ^{226}Ra measured in tuffs and lavas (Trevisi et al., 2005), the heterogeneous distribution of ^{222}Rn concentrations in the volcanic aquifer is likely the result of different processes, including: *i*) leaching of U-rich deposits generated from secondary precipitation of U mobilized from the groundmass of the volcanic rocks and mainly outcropping at the borders of the volcanic system (Locardi and Mittempergher, 1971; Capannesi et al., 2012); *ii*) occurrence and distribution of a significant fracture network, which are expected to be correlated to higher ^{222}Rn concentrations since its mobility increases within fractured rocks (Ball et al., 1991; Vinson et al., 2009); *iii*) aquifer properties, including the contact time between water and aquifer rock, transport processes in the groundwater, differences of transmissivity values, seasonal flow variations, distance to surface waters and/or waters from sedimentary aquifers (Loomis et al., 1988; Ball et al., 1991; Baiocchi et al., 2006). The significantly lower ^{222}Rn concentrations recorded in the thermal waters relative to cold-volcanic waters (Fig. 2d) are likely due to the fast decrease of ^{222}Rn solubility as water temperature increases (Andrews and Woods, 1974; Roba et al., 2010; Clever, 2013). Moreover, as thermal waters are commonly associated with a vigorous CO_2-dominated bubbling gas phase uprising through fractures and faults (Chiodini et al., 1999; Minissale, 2004), the high gas flux may exert a control on the transport of dissolved minor and trace gases, such as ^{222}Rn, being stripped from the solution (Guerra and Etiope, 1999).

6.4 Health hazard evaluation and quality indexes for waters

Actions aimed at mitigating the contamination of the water resources through the removal of As, F^- and ^{222}Rn have become increasingly important. While ^{222}Rn can be efficiently removed (>95%) from water by both aeration and activated carbon filtration (Cothern and Rebers, 2014), several techniques have been developed for the removal of As and F^-, including coagulation-flocculation, ion exchange, adsorption processes, reverse osmosis, membrane filtration and biological processes (e.g., Katsoyiannis and Zouboulis, 2004; Meenakshi and Maheshwari, 2006; Mohan and Pittman, 2007; Vaklavikov et al., 2008; Jagtap et al., 2012). Even the mixing between waters with different concentrations of the pollutants is, where possible, used for remediation. However, none of those techniques turned out to be completely applicable, since all are suffering drawbacks and limitations.

Mitigation actions within the SVD and the VCVD are currently focused only on the removal of As and F^- from drinking waters, while for ^{222}Rn the guidelines issued by the Italian legal provisions (DLgs n° 28/2016) have not still been applied. The occurrence of large sectors of the study area where As and F^- concentrations are largely exceeding the law limits forced policy makers and water resources managers to: *i*) an extensive application of water treatment techniques for their removal and *ii*) the discovery of new water resources of good quality. Water treatment techniques are primarily selected based on their ease of use. The main criticism concerned with the high costs for removal of contaminants, including regeneration and/or disposal of treatment residues, which increase proportionally to the degree of contamination of water.

With the aim to provide a useful tool for water management in a naturally contaminated area, including the discovery of new water resources to be used for human consumption and aimed at ensuring long-term compliance of the resource itself, a quality index (QI) for water samples was defined. QI consists of a number indicating the degree of quality of each sampled water, from the lowest (QI=1) to the highest (QI=4), based on the combined As, F^- and ^{222}Rn concentrations. The parametric approach used for the definition of the QI includes: *i*) identification of hazard concentration thresholds for each element, *ii*) definition of a quality index (QI_x) relative to each

element for each water sample and *iii*) combination of the three QI_x for the calculation of the final QI. The hazard concentration thresholds were established by both considering *i*) the law limits for drinkable waters and *ii*) subjective limits, the latter being based on the concept of acceptable concentration, i.e. a concentration slightly higher than that fixed by law for which remediation interventions aimed at improving the quality of water can reasonably be achieved at low-cost. QI_x values are reported in Tab. 2. For each element, the lower the QI_x value the poorer the quality of water, the latter implying more complex remediation actions. It is noteworthy that the order of magnitude of QI_x is different for each element; this is necessary for the processing of the final QI distribution map, in which each water sample is represented by three digits, the first one representing the QI_x of ^{222}Rn, the second that of F^- and the third one that of As. The resulting QI distribution map is reported in Fig. 6. Arsenic is the key parameter used to define the final QI of each water sample (Tab. 3), basically because its toxicity is higher than that of F^- and ^{222}Rn at the concentrations measured in the study area and the treatment plants for its removal are more expensive. In the map, the areas showing QI=1 refer to low and very low quality waters for human consumption, since As concentrations (>50 μg/L) are considerably exceeding the limit fixed by law (10 μg/L). Very low-quality waters (Fig. 6; Tab. 3), representing about the 77% of the total of this group, also have high F^- concentrations (>1.5 mg/L) and, less frequently, high ^{222}Rn concentrations (about the 21%). Remediation actions could generally be complex and expensive. Areas with QI=2 are characterized by low-to-medium quality waters, basically fixed by As concentrations within the range 20.1–50 μg/L (Tab. 2). More than half of the waters of this group have F^- concentrations higher than the law limits, whereas for about one third of the total database As is the only contaminant exceeding the law limits (medium-to-low quality waters; Fig. 6). As already stated, water treatments for the removal of contaminants are necessarily more or less complex and expensive according to *i*) As concentration and *ii*) occurrence of high F^- (and sometimes ^{222}Rn) concentrations. Areas with QI=3 are characterized by medium and medium-to-high quality waters fixed by As concentrations within the range 10.1–20 μg/L. Medium quality waters are those

characterized by F^- concentrations (about the 25% of the total) or ^{222}Rn concentrations (about the 20%) above the law/recommended limits, while medium-to-high quality waters are those for which remediation actions can be planned limitedly to the As concentrations. Areas with QI=4 are fixed by As concentrations <10 μg/L, i.e. below the law limit for human consumption. This group includes high- and very high-quality waters (Fig. 6), the latter including about the 84% of the total, and a few waters characterized by F^- or ^{222}Rn concentrations higher than the law/recommended limits (about the 5% and 11%, respectively). The latter can still be considered high quality waters, basically because water treatments do not involve As. It is noteworthy that F^- concentrations within the optimum range for human health (0.50-1.50 mg/L) are only represented by 31% of high-quality waters, while for the remaining 69% the concentrations are within the quality standards for human consumption but below 0.50 mg/L. Despite waters hosted in the sedimentary aquifers are characterized by high QI (Fig. 6), due to their modest thickness and limited lateral extension, their use for water supply purposes is difficult and/or limited to few potential users. On the other hand, the surface of areas characterized by high quality waters (QI=4) drastically decreases within the sectors occupied by volcanic deposits, which are those hosting the regional cold aquifer which is the only that can be exploited for the drinking water supply. Within the VCVD, suitable water resources (QI=4) for supplying drinking waters can be identified in the north-eastern sector, which includes the Cimini mountains and houses from several villages and urban centers including Orte (~9,000 inhabitants). Medium-to-high quality waters (QI=3) could also be potentially suitable for human consumption if treated through low-cost removal techniques, such as mixing with non-contaminated waters that can be considered a valid alternative to de-arsenification. Within the SVD, high quality waters occur in the northern sector between Bassano and Monterosi, east of Bracciano Lake and in the north-eastern sector between Magliano and Faleria (Fig. 1). Medium-to-high quality waters can also be found in the surrounding areas.

7. Concluding remarks

492 The spatial distribution maps of As, F^- and ^{222}Rn in the volcanic-sedimentary aquifers of the
493 SVD and the VCVD were drawn on the geochemical data collected from (municipal, domestic)
494 wells and springs during extensive sampling surveys. Contour maps produced by the application of
495 geostatistical methods showed that severe As and, to a lesser extent, F^- contamination affect the
496 water resources in wide sectors within the study area. More than 60% of waters hosted in the
497 volcanic rock aquifer, i.e. the one that provides drinking water for local inhabitants, had As
498 concentrations exceeding the value allowed for human consumption. In the case of F^- the
499 percentage reduced to approximately 25%. Geogenic contamination of waters hosted in the volcanic
500 rocks is mainly caused by mixing with As- and F-rich fluids uprising through faulted and fractures
501 zones from a deep hydrothermal reservoir. High As and F^- concentrations in the thermal waters are
502 related to water-rock interaction processes at high temperature that enhance the mobility of these
503 contaminants. Conversely, cold waters interacting with volcanic rocks produced lower As and F^-
504 concentrations in the sectors of the volcanic aquifer characterized by the lack of structural
505 elements that prevents the uprising of fluids from the hydrothermal reservoir. Lithology is
506 likely the main factor controlling the ^{222}Rn distribution in the study area. Significantly higher
507 concentrations were measured in waters hosted in the volcanic aquifer with respect to those
508 measured in waters circulating within the sedimentary units, as consequence of the relatively high
509 concentration of Rn-generating radionuclides in the volcanic rocks. The low ^{222}Rn concentrations
510 measured in thermal waters are likely related to the rapid decrease of Rn solubility in water as
511 temperature increases. In terms of potential health risks due to the direct ingestion of Rn-rich
512 waters, approximately 22% of those circulating in the volcanic rocks exceed the recommended
513 value for human consumption.
514 Since waters hosted in the sedimentary units do not represent important resources for human
515 consumption, due to their limited availability, the deterioration of water resources within the
516 volcanic aquifer poses a serious public health problem for policy makers. Unfortunately, current
517 practices for the removal geogenic contaminants from water are expensive and not fully applicable

518 to all situations. Moreover, they do not guarantee long-term compliances of drinking waters. On this
519 basis, the processing of the acquired dataset for the definition of a quality index (QI) for each
520 individual water sample and the construction of a QI distribution map may represent, coupled with
521 an exhaustive description of the spatial distribution of the single contaminants, an essential source
522 of information for the development of intervention plans aimed at discovering new water resources
523 for human consumption and mitigating the impact on groundwater quality.
524
525 **References**
526 Acocella, V., Funiciello, R., 2006. Transverse systems along the extensional Tyrrhenian margin of
527 central Italy and their influence on volcanism. Tectonics 25, doi: 10.1029/2005TC001845.
528 Aiuppa, A., Allard, P., D'Alessandro, W., Michel, A., Parello, F., Treuil, M., Valenza, M., 2000.
529 Mobility and fluxes of major, minor and trace metals during basalt weathering and groundwater
530 transport at Mt. Etna volcano (Sicily). Geochim. Cosmochim. Acta 64, 1827-1841.
531 Aiuppa, A., D'Alessandro, W., Federico, C., Palumbo, B., Valenza, M., 2003. The aquatic
532 geochemistry of arsenic in volcanic groundwaters from southern Italy. Appl. Geochem. 18, 1283-
533 1296.
534 Aiuppa, A., Federico, C., Allard, P., Gurrieri, S., Valenza, M., 2005. Trace metal modeling of
535 groundwater-gas-rock interactions in a volcanic aquifer: Mount Vesuvius, southern Italy. Chem.
536 Geol. 216, 289-311.
537 Aiuppa, A., Avino, R., Brusca, L., Caliro, S., Chiodini, G., D'Alessandro, W., Favara, R., Federico,
538 C., Ginevra, W., Inguaggiato, S., Longo, M., Pecoraino, G., Valenza, M., 2006. Mineral control of
539 arsenic content in thermal waters from volcano-hosted hydrothermal systems: insights from island
540 of Ischia and Phlegrean Fields (Campanian Volcanic Province, Italy). Chem. Geol. 229, 313-330.
541 Allard, P., Aiuppa, A., Loyer, H., Carrot, F., Gaudry, A., Pinte, G., Michel, A., Dongarrà, G., 2000.
542 Emission rate of metals and acid gases during long-lived basalt degassing at Stromboli volcano.
543 Geophys. Res. Lett. 27, 1207-1210.

544 Alonso, H., Cruz-Fuentes, T., Rubiano, J.G., González-Guerra, J., del Carmen Cabrera, M., Arnedo,
545 M.A.,Tejera, A., Rodríguez-Gonzalez, A., Pérez-Torrado, F.J., Martel, P., 2015. Radon in
546 groundwater of the northeastern Gran Canaria aquifer. Water 7, 2575-2590.
547 Andrews, J.N., Wood, D.F., 1974. Radium 226, radon 222 and lead 210 in bath thermal springs
548 compared with some environmental waters. Health Phys. 27, 307-310.
549 Angelone, M., Cremisini, C., Piscopo, V., Proposito, M., Spaziani, F., 2009. Influence of
550 hydrostratigraphy and structural setting on the arsenic occurrence in groundwater of the Cimino-
551 Vico volcanic area (central Italy). Hydrogeol. J. 17, 901-914.
552 Armiento, G., Baiocchi, A., Cremisini, C., Crovato, C., Lotti, F., Lucentini, L., Mazzuoli, M.,
553 Nardi, E., Piscopo, V., Proposito, M., Veschetti, E., 2015. An integrated approach to identify water
554 resources for human consumption in an area affected by high natural arsenic content. Water 7,
555 5091-5114.
556 Baiocchi, A., Coletta, A., Espositi, L., Lotti, F., Piscopo, V., 2013. Sustainable groundwater
557 development in a naturally arsenic-contaminated aquifer: the case of the Cimino-Vico volcanic area
558 (central Italy). Ital. J. Eng. Geol. Environ., doi: 10.4408/IJEGE.2013-01.O-01.
559 Baiocchi, A., Dragoni, W., Lotti, F., Luzzi, G., Piscopo, V., 2006. Outline of the hydrogeology of
560 the Cimino and Vico volcanic area and of the interaction between groundwater and lake Vico
561 (Lazio Region, central Italy). Boll. Soc. Geol. It. 125, 187-202.
562 Baldi, P., Decandia, F.A., Lazzarotto, A., Calamai, A., 1974. Studio geologico del substrato della
563 copertura vulcanica laziale delle zone dei laghi di Bolsena, Vico e Bracciano. Mem. Soc. Geol. It.
564 13, 575-606.
565 Ball, T.K., Cameron, D.G., Colman, T.B., Roberts, P.D., 1991. Behaviour of radon in the geological
566 environment: a review. Quart. J. Eng. Geol. 24, 169-182.
567 Ballantyne, J.M., Moore, J.N., 1988. Arsenic geochemistry in geothermal systems. Geochim.
568 Cosmochim. Acta 52, 475-483.

569 Barberi, F., Buonasorte, G., Cioni, R., Fiordelisi, A., Foresi, L., Iaccarino, S., Laurenzi, M.A.,
570 Sbrana, A., Vernia, L., Villa, I.M., 1994. Plio-Pleistocene geological evolution of the geothermal
571 area of Tuscany and Latium. Mem. Descr. Carta Geol. Ital. 49, 77-134.
572 Barnes, H.L. (Ed.), 1977. Geochemistry of hydrothermal ore deposits, 3rd edition. Wiley and Sons,
573 New York, USA.
574 Bissen, M., Frimmel, F.H., 2003. Arsenic: a review – part I – occurrence, toxicity, speciation,
575 mobility. Acta Hydroc. Hydrob. 31, 9-18.
576 Bundschuh, J., Armienta, M.A., Birkle, P., Bhattacharya, P., Matschullat, J., Mukherjee, A.B.
577 (Eds.), 2009. Natural arsenic in groundwaters of Latin America. Taylor & Francis, London, UK.
578 Capannesi, G., Rosada, A., Manigrasso, M., Avino, P., 2012. Rare earth elements, thorium and
579 uranium in ores of the North-Latium (Italy). J. Radioanal. Nucl. Chem. 291, 163-168.
580 Capelli, G., Mazza, R., Gazzetti, C., 2005. Strumenti e strategie per la tutela e l'uso compatibile
581 della risorsa idrica nel Lazio: gli acquiferi vulcanici. Ed. Pitagora.
582 Chiodini, G., Frondini, F., Kerrick, D.M., Rogie, J., Parello, F., Peruzzi, L., Zanzari, A.R., 1999.
583 Quantification of deep CO_2 fluxes from central Italy. Examples of carbon balance for regional
584 aquifers and of soil diffuse degassing. Chem. Geol. 159, 205-222.
585 Choubisa, S.L., 1999. Chronic fluoride intoxication (fluorosis) in tribes and their domestic animals.
586 Int. J. Environ. Stud. 36, 703-716.
587 Cimarelli C., De Rita D., 2006. Structural evolution of the Pleistocene Cimini trachytic volcanic
588 complex (Central Italy). Bull Volcanol 68, 538-548.
589 Cinti, D., Poncia, P.P., Brusca, L., Tassi, F., Quattrocchi, F., Vaselli, O., 2015. Spatial distribution
590 of arsenic, uranium and vanadium in the volcanic-sedimentary aquifers of the Vicano-Cimino
591 Volcanic District (central Italy). J. Geochem. Explor. 152, 123-133.
592 Cinti, D., Poncia, P.P., Procesi, M., Galli, G., Quattrocchi, F., 2013. Geostatistical techniques
593 application to dissolved radon hazard mapping: an example from the western sector of the Sabatini
594 volcanic district and the Tolfa Mountains (central Italy). Appl. Geochem. 35, 312-324.

595 Cinti, D., Procesi, M., Tassi, F., Montegrossi, G., Sciarra, A., Vaselli, O., Quattrocchi, F., 2011.
596 Fluid geochemistry and geothermometry in the western sector of the Sabatini volcanic district and
597 the Tolfa mountains (central Italy). Chem. Geol. 284, 160-181.
598 Cinti, D., Tassi, F., Procesi, M., Bonini, M., Capecchiacci, F., Voltattorni, N., Vaselli, O.,
599 Quattrocchi, F., 2014. Fluid geochemistry and geothermometry in the unexploited geothermal field
600 of the Vicano-Cimino volcanic district (central Italy). Chem. Geol. 371, 96-114.
601 Cinti, D., Tassi, F., Procesi, M., Brusca, L., Cabassi, J., Capecchiacci, F., Delgado Huertas, A.,
602 Galli, G., Grassa, F., Vaselli, O., Voltattorni, N., 2017. Geochemistry of hydrothermal fluids from
603 the eastern sector of the Sabatini volcanic district (central Italy). Appl. Geochem. 84, 187-201.
604 Cioni, R., Laurenzi, M.A., Sbrana, A., Villa, I.M., 1993. ^{40}Ar-^{39}Ar chronostratigraphy of the initial
605 activity in the Sabatini Volcanic Complex (Italy). Boll. Soc. Geol. It. 112, 251-263.
606 Clever, H.L., 2013. IUPAC Solubility Data Series. Krypton, Xenon and Radon - Gas Solubilities,
607 vol. 2. Pergamon Press, Oxford, UK, 378 pp.
608 Conticelli, S., Peccerillo, A., 1992. Petrology and geochemistry of potassic and ultrapotassic
609 volcanism in central Italy: petrogenesis and inferences on the evolution of the mantle sources.
610 Lithos 28, 221-240.
611 Cothern, C.R., Rebers, P.A., 2014. Radon, radium and uranium in drinking water. Lewis Publishers,
612 New York.
613 Council Directive 98/83/EC of 3 November 1998. European Commission, Brussels
614 (http://eur-lex.europa.eu/LexUriServ/LexUriServ.do?uri=OJ:L:1998:330:0032:0054:EN:PDF).
615 Council Directive 2013/51/EURATOM of 22 October 2013. European Commission, Brussels
616 (http://eur-lex.europa.eu/legal-content/EN/TXT/PDF/?uri=CELEX:32013L0051&from=EN)
617 D'Alessandro, W., 2006. Human fluorosis related to volcanic activity: a review. In: Kungolos,
618 A.G., Brebbia, C.A., Samaras, C.P., Popov, V. (Eds.) Environmental Toxicology. WIT Press,
619 Southampton, UK, pp. 21-30.

620 Dall'Aglio, M., Giuliano, G., Amicizia, D., Andrenelli, M.C., Cicioni, G.B., Mastroianni, D.,
621 Sepicacchi, L., Tersigni, S., 2001. Assessing drinking water quality in northern Latium by trace
622 elements analysis. In: Cidu, R. (Ed.), Proc. of the 10th Int. Symp. on Water-Rock Interaction,
623 Villasimius, Italy, pp. 1063-1066.
624 Della Vedova, B., Bellani, S., Pellis, G., Squarci, P., 2001. Deep temperatures and surface heat flow
625 distribution. In: Vai, G.B., Martini, P. (Eds.), Anatomy of an orogen: the Apennines and adjacent
626 Mediterranean basins 65-76.
627 De Rita, D., Cremisini, C., Cinnirella, A., Spaziani, F., 2011. Fluorine in the rocks and sediments of
628 volcanic areas in central Italy: total content, enrichment and leaching processes and a hypothesis on
629 the vulnerability of the related aquifers. Environ. Monit. Assess. 184, 5781-5796.
630 De Rita, D., Di Filippo, M., Rosa, C., 1996. Structural evolution of the Bracciano volcano-tectonic
631 depression, Sabatini Volcanic District, Italy. In: McGuire, W.C. et al. (Eds.), Volcano Instability on
632 the Earth and Other Planets, Geol. Soc. Spec. Publication, 110, 225-236.
633 Dubois, G., 2005. "An overview of radon survey in Europe". Radioactivity Environmental
634 Monitoring Emissions and Health Unit Institute for Environment and Sustainability JRC –
635 European Commission. EUR 21892 EN, EC, 168 pp.
636 Edmunds, W.M., Smedley, P.L., 1996. Groundwater geochemistry and health: an overview. In:
637 Appleton, JD., Fuge, R., McCall, G.J.H. (Eds.), Environmental Geochemistry and Health,
638 Geological Society Special Publ. 113.
639 Ellis, A.J., Mahon, W.A.J., 1977. Chemistry and geothermal systems. Academic Press, New York.
640 Fabiani, L., Leoni, V., Vitali, M., 1999. Bone-fracture incidence rate in two Italian regions with
641 different fluoride concentration levels in drinking water. J. Trace Elements Med. Biol. 13, 232-237.
642 Faure, G., 1991. Principles and applications of inorganic geochemistry. MacMillan Publ. Co., New
643 York, NT, pp. 626.
644 Fradà, G., Mentesana, G., Guaijani, U., 1969. Thyroid function in endemic hydrofluorosis in Sicily.
645 Fluoride 2, 195-200.

646 Goovaerts, P., 1997. Geostatistics for Natural Resources Evaluation. New York; Oxford University
647 Press.
648 Guerra, M., Etiope, G., 1999. Effects of gas-water portioning, stripping and channelling processes
649 on radon and helium distribution in fault areas. Geochem. J. 33, 141-151.
650 Guo, H., Wang, Y., 2005. Geochemical characteristics of shallow groundwater in Datong basin,
651 northwestern China. J. Geochem. Explor. 87, 109-120.
652 Hopke, P.K., Borak, T.B., Doull, J., Cleaver, E., Eckerman, K.F., Gundersen, L.C.S., Harley, N.H.,
653 Hess, C.T., Kinner, N.E., Kopecky, K.J., McKone, T.E., Sextro, R.G., Simon, S.L., 2000. Health
654 risks due to radon in drinking water. Environ. Sci. Technol. 34, 921-926.
655 IARC, 2004. International Agency for Research on Cancer. IARC monographs on the evaluation of
656 carcinogenic risks to humans. Volume 84. Some drinking-water disinfectants and contaminants,
657 including arsenic. Lyon.
658 Jagtap, S., Yenkie, M.K., Labhsetwar, N., Rayalu, S., 2012. Fluoride in drinking water and
659 defluoridation of water. Chem. Rev. 112, 2454-2466.
660 Katsoyiannis, I.A., Zouboulis A.I., 2004. Application of biological processes for the removal of
661 arsenic from groundwaters. Water Res. 38, 17-26.
662 Krige, D.G., 1966. Two dimensional weighted moving average trend surfaces for ore-evaluation. J.
663 S. Afr. Inst. Min. Metall. 66, 13-38.
664 Laurenzi, M.A., Villa, I.M., 1987. $^{40}Ar/^{39}Ar$ chronostratigraphy of Vico ignimbrites. Period.
665 Mineral. 56, 285-293.
666 Locardi, E., Mittempergher, M., 1971. Exhalative supergenic uranium, thorium and marcasite
667 occurrences in quaternary volcanites of central Italy. Bull. Volcanol. 35, 173-184.
668 Loomis, D.P., Watson, J.E., Crawford-Brown, D.J., 1988. Predicting the occurrence of radon-222 in
669 groundwater supplies. Environ. Geochem. Health 10, 41-50.
670 Manca, F., Viaroli, S., Mazza, R., 2017. Hydrogeology of the Sabatini Volcanic District (central
671 Italy). J. Maps 13, 252-259.

672 Mancini, C., Quattrocchi, F., Guadoni, F., Pizzino, L., Porfidia, B., 2000. ^{222}Rn study throughout
673 different seismotectonical areas: comparison between different techniques for discrete monitoring.
674 Ann. Geofis. 43, 1-28.
675 Marra F., Karner, D.B., Freda, C., Gaeta, M., Renne, P. (2009). Large mafic eruptions at Alban
676 Hills Volcanic District (central Italy): chronostratigraphy, petrography and eruptive behavior. J.
677 Volcanol. Geotherm. Res. 179, 217-232.
678 Matheron, G., 1971. The theory of regionalized variables and its applications. Cahiers du Centre de
679 Morphologie Mathematique, Fontainbleau.
680 Meenakshi, S., Maheshwari, R.C., 2006. Fluoride in drinking water and its removal. J. Hazard
681 Mater. 37, 456-463.
682 Minissale, A., 2004. Origin, transport and discharge of CO2 in central Italy. Earth-Sci. Rev. 66, 89-
683 141.
684 Mohan, D., Pittman, C.U., 2007. Arsenic removal from water/wastewater using adsorbents – a
685 critical review. J. Hazard. Mater. 142, 1-53.
686 Nordstrom, D.K., 2002. Worldwide occurrences of arsenic in ground water. Science 296, 2143-
687 2145.
688 Oremland, R.S., Stolz, J.F., 2003. The ecology of arsenic. Science 300, 939-944.
689 Ozsvath, D.L., 2009. Fluoride and environmental health: a review. Rev. Environ. Sci. Biotechnol. 8,
690 59-79.
691 Paone, A., Ayuso, R.A., De Vivo, B., 2001. A metallogenic survey of alkalic rocks of Mt. Somma-
692 Vesuvius volcano. Mineral. Petrol. 73, 201-233.
693 Peccerillo, A., 2017. Cenozoic volcanism in the Tyrrhenian Sea region. Springer International
694 Publishing AG, Cham, Switzerland.
695 Piscopo, V., Armiento, G., Baiocchi, A., Mazzuoli, M., Nardi, E., Piacentini, S.M., proposito, M.,
696 Spaziani, F., 2018. Role of high-elevation groundwater flows in the hydrogeology of the Cimino

volcano (central Italy) and possibilities to capture drinking water in a geogenically contaminated environment. Hydrogeol. J., doi: 10.1007/s10040-017-1718-6.

Preziosi, E., Rossi, D., Parrone, D., Ghergo, S., 2016. Grounfwater chemical status assessment considering geochemical background: an example from northern Latium (central Italy). Rend. Fis. Acc. Lincei 27, 59-66.

Rahman, M.M., Sengupta, M.K., Ahamed, S., Chowdhury, U.K., Hossain, M.A., Das, B., Lodh, D., Saha, K.C., Pati, S., Kaies, I., Barua, A.K., Chakraborti, D., 2005. The magnitude of arsenic contamination in groundwater and its health effects to the inhabitants of the Jalangi: one of the 85 arsenic affected blocks in West Bengal, India. Sci. Total Environ. 338, 189-200.

Ravenscroft, P., Brammer, H., Richards, K. (Eds.), 2009. Arsenic pollution: a global synthesis. John Wiley & Sons, West Sussex, UK.

Reimann, C., Bjorvatn, K., Frengstad, B., Melaku, Z., Tekle-Haimanot, R., Siewers, U., 2003. Drinking water quality in the Ethiopian section of the East African Rift Valley I – data and health aspects. Sci. Total Environ. 311, 65-80.

Ren, F.R., Shugin, J., 1988. Distribution and formation of high-fluorine groundwater in China. Environ. Geol. Water Sci. 12, 3-10.

Roba, C.A., Codrea, V., Moldovan, M., Baciu, C., Cosma, C., 2000. Radium and radon content of some cold and thermal aquifers from Bihor country (northwestern Romania). Geofluids 10, 571-585.

Sawyer, G.M., Opperheimer, C., 2006. Volcanic fluorine emissions: observations by Fourier transform infrared spectroscopy. In: Tressaud, A. (Ed.) Fluorine and the environment: atmospheric chemistry, emissions, and lithosphere. Elsevier, Amsterdam, The Netherlands.

Scrocca, D., Doglioni, C., Innocenti, F., 2003. Constraints for an interpretation of the Italian geodynamics: a review. Mem. Descr. Carta Geol. D'It. 62, 15-46.

721 Serri, G., Innocenti, F., Manetti, P., 1993. Geochemical and petrological evidence of the subduction
722 of delaminated Adriatic continental lithosphere in the genesis of the Neogene-Quaternary
723 magmatism of central Italy. Tectonophysics 223, 117-147.
724 Smedley, P.L., Kinniburgh, D.G., 2002. A review of the source, behavior and distribution of arsenic
725 in natural waters. Appl. Geochem. 17, 517-568.
726 Soto-Rojas, A.E., Ureña-Cirett, J.L., Martínez-Mier, E.A., 2004. A review of the prevalence of
727 dental fluorosis in Mexico. Pan Am. J. Public Health 15, 9-17.
728 Synnott, H., Fenton, D., 2005. An evaluation of radon reference levels and radon measurement
729 techniques and protocols in European Countries. ERRICCA 2 Report. European Commission
730 Contract No: FIRI-CT-2001-20142.
731 Trevisi, R., Bruno, M., Orlando, C., Ocone, R., Paolelli, C., Amici, M., Altieri, A., Antonelli, B.,
732 2005. Radiometric characterization of more representative natural building materials in the province
733 of Rome. Radiat. Protect. Dosim. 113, 168-172.
734 UNSCEAR (United Nations Scientific Committee on the Effects of Atomic Radiation), 2008.
735 Sources and effects of ionizing radiation. Report to General Assembly, Annex B, United Nations,
736 New York City, NY, USA, 245 pp.
737 Vaklavikov, M., Gallios, G.P., Hredzak, S., Jakabsky, S., 2008. Removal of arsenic from water
738 streams: an overview of available techniques. Clean Techn. Environ. Policy 10, 89-95.
739 Webster, J.G., Nordstrom, D.K., 2003. Geothermal arsenic. In: Welch, A.H., Stollenwerk, K.G.
740 (Eds.) Arsenic in Groundwater, Geochemistry and Occurrence. Kluvert, The Netherlands, pp. 101-
741 112.
742 Weinstein, L.H., Davison, A., 2003. Fluoride in the environment, CABI Publishing, Wallingford,
743 UK.
744 WHO, 2011. Guidelines for drinking-water quality, 4th ed. Geneva: WHO Press.

745 Viaroli, S., Cuoco, E., Mazza, R., Tedesco, D., 2016. Dynamics of natural contamination by
746 aluminum and iron rich colloids in the volcanic aquifers of central Italy. Environ. Sci. Pollut. Res.
747 23, 19958-19977.
748 Vinson, D.S., Vengosh, A., Hirschfeld, D., Dwyer, G.S., 2009. Relationships between radium and
749 radon occurrence and hydrochemistry in fresh groundwater from fractured crystalline rocks, North
750 Carolina (USA). Chem. Geol. 260, 159-171.
751 Vivona, R., Preziosi, E., Madé, B., Giuliano, G., 2007. Occurrence of minor toxic elements in
752 volcanic-sedimentary aquifers: a case study in central Italy. Hydrogeol. J. 15, 1183-1196.
753 Voltaggio, M., Di Lisa, G.A., Voltaggio, S., 2001. U-series disequilibrium study on a gaseous
754 discharge area (Solforata di Pomezia, Alban Hills, Italy): implications for volcanic and geochemical
755 risk. Appl. Geochem. 16, 57-72.
756

757 **Table captions**

758 Table 1 - Basic statistics relative to the whole population of samples and subsets of the whole
759 population defined on the basis of the water type (cold or thermal) and the aquifer rock (volcanic or
760 sedimentary). Concentrations are expressed as μg/L (As), mg/L (F^-) and Bq/L (^{222}Rn).
761

762 Table 2 – QI_x values for the selected elements. Concentration ranges are expressed as μg/L for As,
763 mg/L for F^- and Bq/L for ^{222}Rn.
764

765 Table 3 – Possible combinations of the partial quality indexes for the final QI processing. The QI_{As}
766 was considered as the main parameter for the definition of the global QI of each sampled water.
767

768 **Figure captions**

769 Figure 1 – a) Geological sketch map of the SVD and the VCVD with the location of the collected
770 waters and b) simplified geological model. The potentiometric surface of the basal aquifer is taken
771 from Capelli et al. (2005).
772
773 Figure 2 - Box plot of the subsets of the whole sampling population for As (a, b), F^- (c) and ^{222}Rn
774 (d).
775
776 Figure 3 –Map of the spatial distribution of As (μg/L) in the aquifers of the SVD and VCVD as
777 obtained from ordinary kriging after back-transformation into original variable values.
778
779 Figure 4 – Map of the spatial distribution of F^- (mg/L) in the aquifers of the SVD and VCVD as
780 obtained from ordinary kriging after back-transformation into original variable values.
781
782 Figure 5 - Map of the spatial distribution of dissolved ^{222}Rn (Bq/L) in the aquifers of the SVD and
783 VCVD as obtained from ordinary kriging after back-transformation into original variable values.
784
785 Figure 6 – Contour map of the quality indexes processed by combining the concentrations of As, F^-
786 and ^{222}Rn of the collected waters.
787
788 **Supplementary material**
789 Supplementary Material 1 – As (in μg/L), F^- (in mg/L) and ^{222}Rn concentrations (in Bq/L) of the
790 collected waters. Legend: s = spring, w = well, p = bubbling pool, CS = cold sedimentary, CV =
791 cold volcanic, TW = thermal water; n.a. = not analyzed. *Data from Vivona et al. (2007).
792
793 Supplementary material 2 – Geological sketch map of the SVD and the VCVD reporting labelled
794 sampling points. For the legend see Fig. 1.

Supplementary material 3 – QQ-plots of the As, F^- and ^{222}Rn concentrations for the whole population of samples and subsets. Comparison between original and log-transformed variables.

Supplementary material 4 - Experimental directional semi-variogram of the transformed As concentrations for the collected waters.

Supplementary material 5 - Experimental directional semi-variogram of the transformed F^- concentrations for the collected waters.

Supplementary material 6 - Experimental directional semi-variogram of the transformed ^{222}Rn concentrations for the collected waters.

Supplementary material 7 – Experimental semi-variogram parameters, structural model parameters, cross-validation results and neighborhood parameters for As, F^- and ^{222}Rn datasets.

a)

VICANO-CIMINO VOLCANIC DISTRICT

TOLFA MOUNTAINS

SABATINI VOLCANIC DISTRICT

N

TUSCANIA

VITERBO

Cimini

ORTE

Vico Lake

NEPI

FIANO

Bracciano Lake

ANGUILLARA

Tevere River

Tolfa

Ceriti

CIVITAVECCHIA

TYRRHENIAN SEA

200 300 400 500 400 300 200 100 400 100 150 200 300 250 200 150 100 50

0 5 10 20 Km

TUFFS
LAVAS
Volcanic units (Pleistocene)

LAVA DOMES (Pleistocene)

CLAYS (Plio-Pleistocene)

CONGLOMERATES (Mio-Pliocene)

LIGURIAN s.l. (Creta-Oligocene)

CARBONATES (Mesozoic)

ANHYDRITES (Triassic)

TRAVERTINES (Holoc.-Pleistocene)

ALLUVIAL DEPOSITS (Holocene)

CO_2-RICH COLD WATERS

THERMAL WATERS

COLD WATERS

100 CONTOUR LINES OF THE VOLCANIC AQUIFER

b)

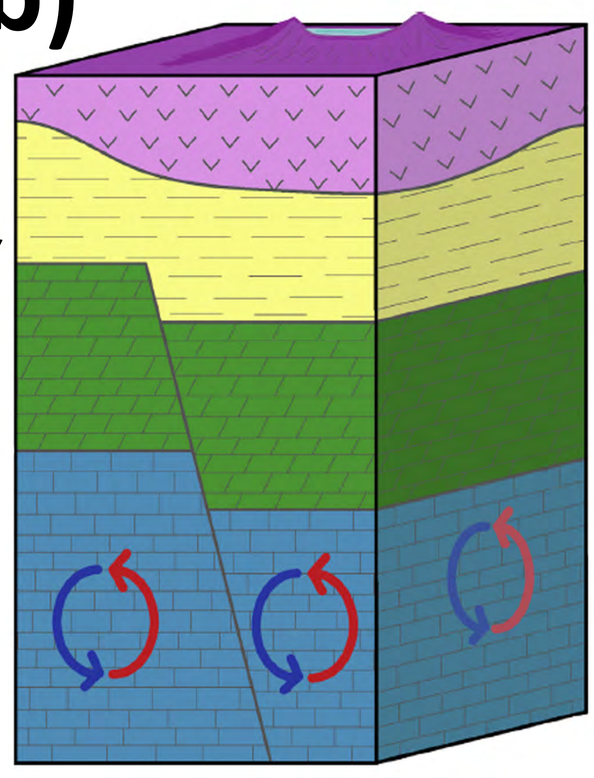

a)

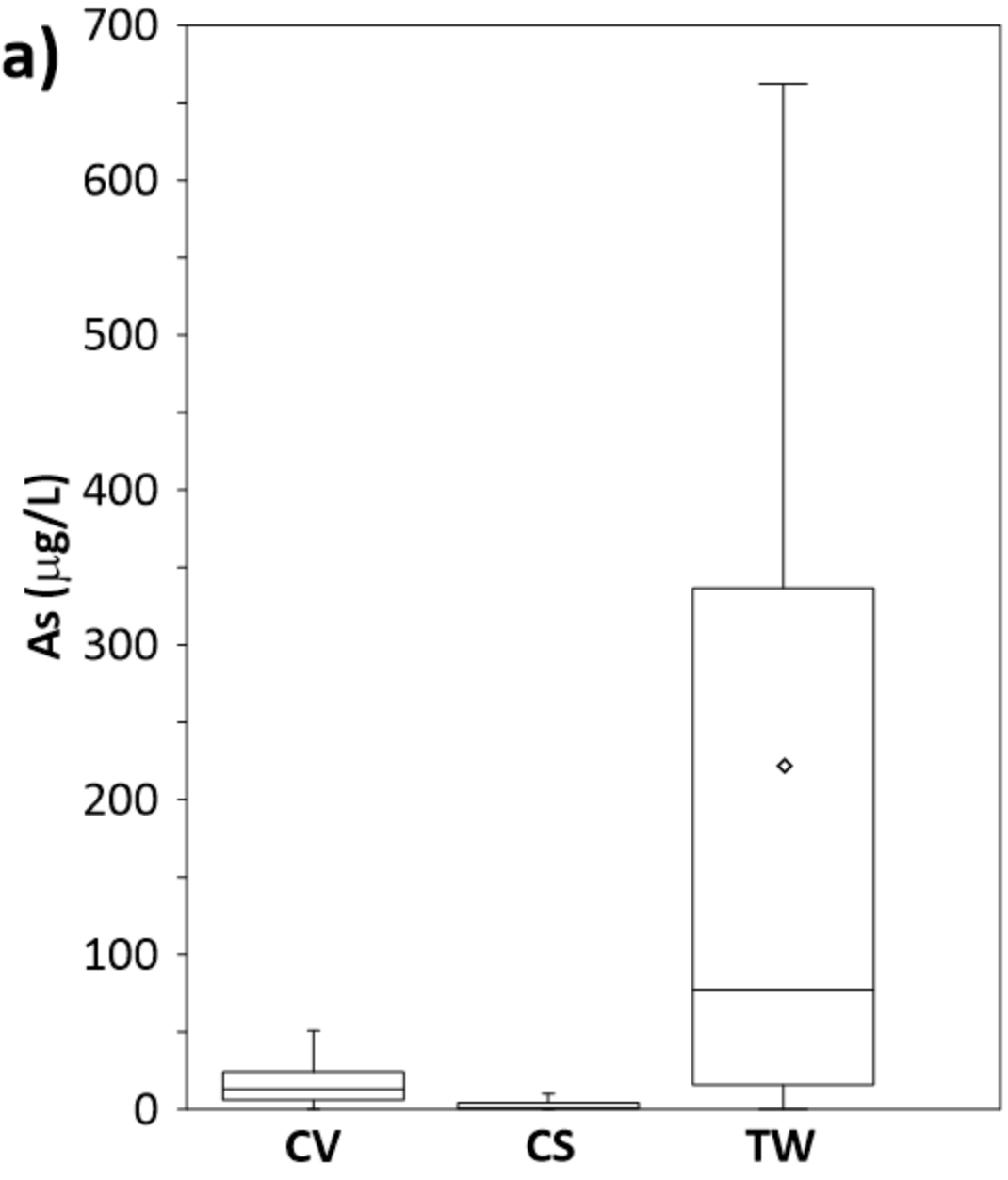
As (µg/L)
700
600
500
400
300
200
100
0
CV
CS
TW

b)

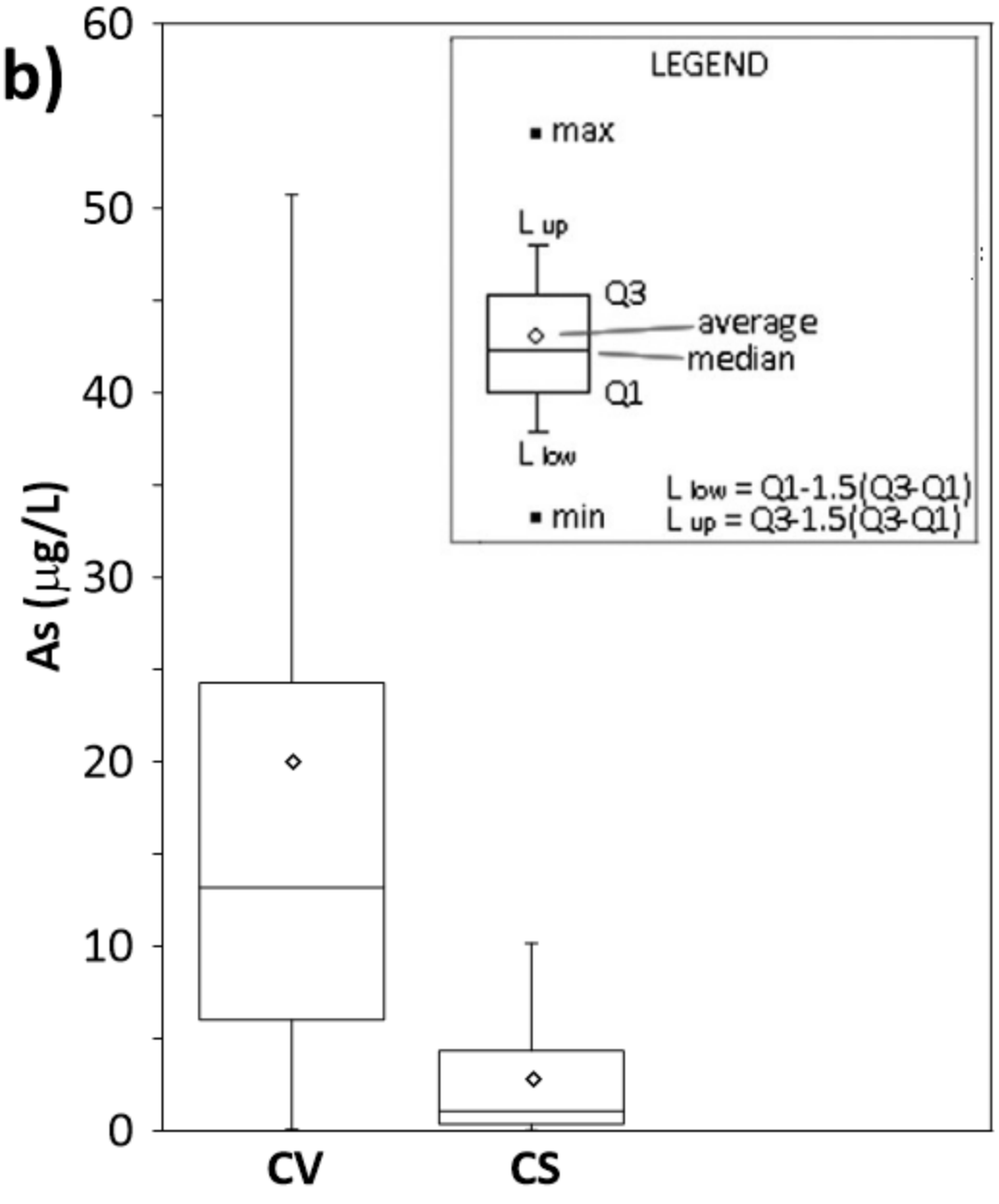
As (µg/L)
60
50
40
30
20
10
0
CV
CS
LEGEND
max
L up
Q3
average
median
Q1
L low
min
L low = Q1-1.5(Q3-Q1)
L up = Q3-1.5(Q3-Q1)

c)

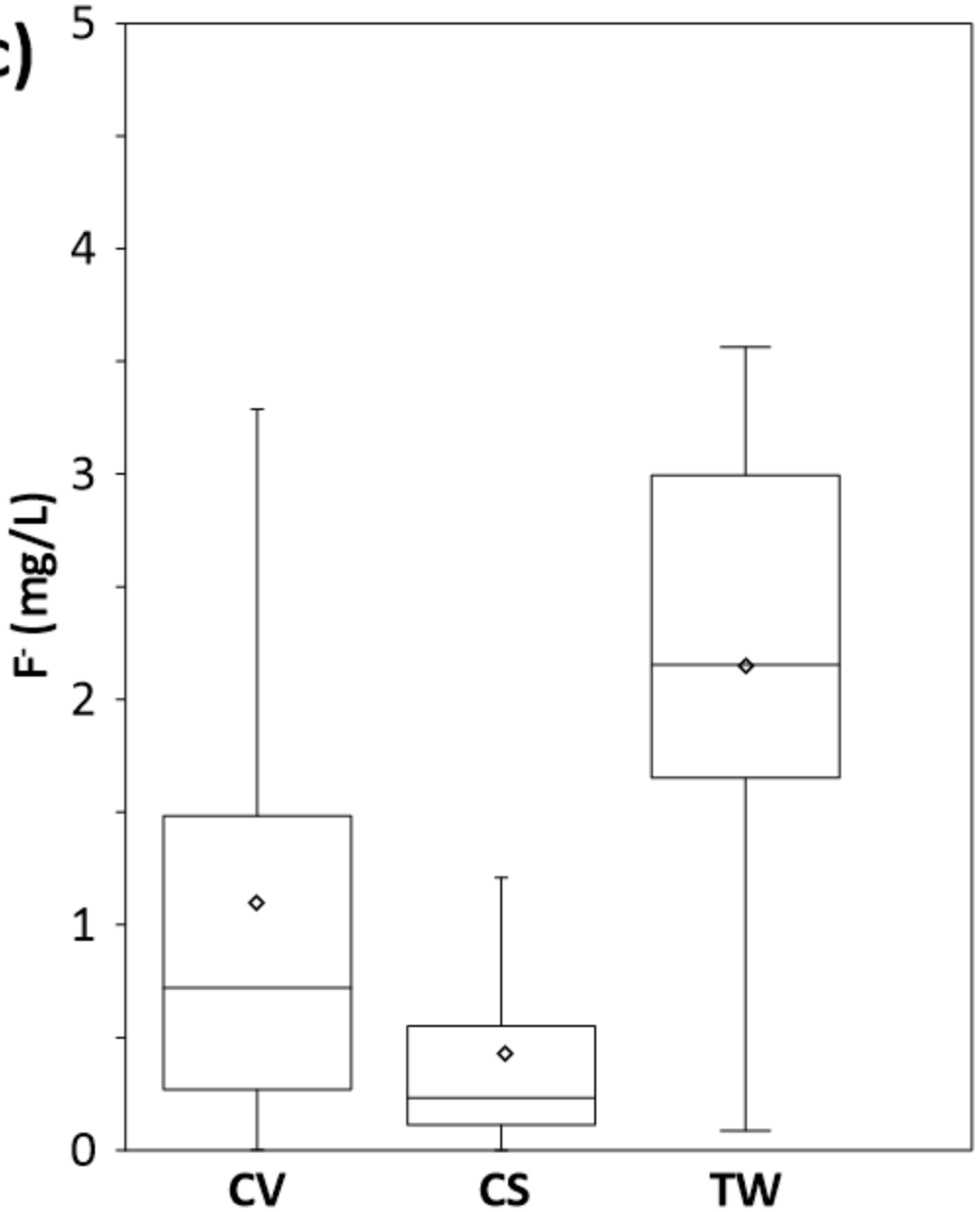
F- (mg/L)
5
4
3
2
1
0
CV
CS
TW

d)

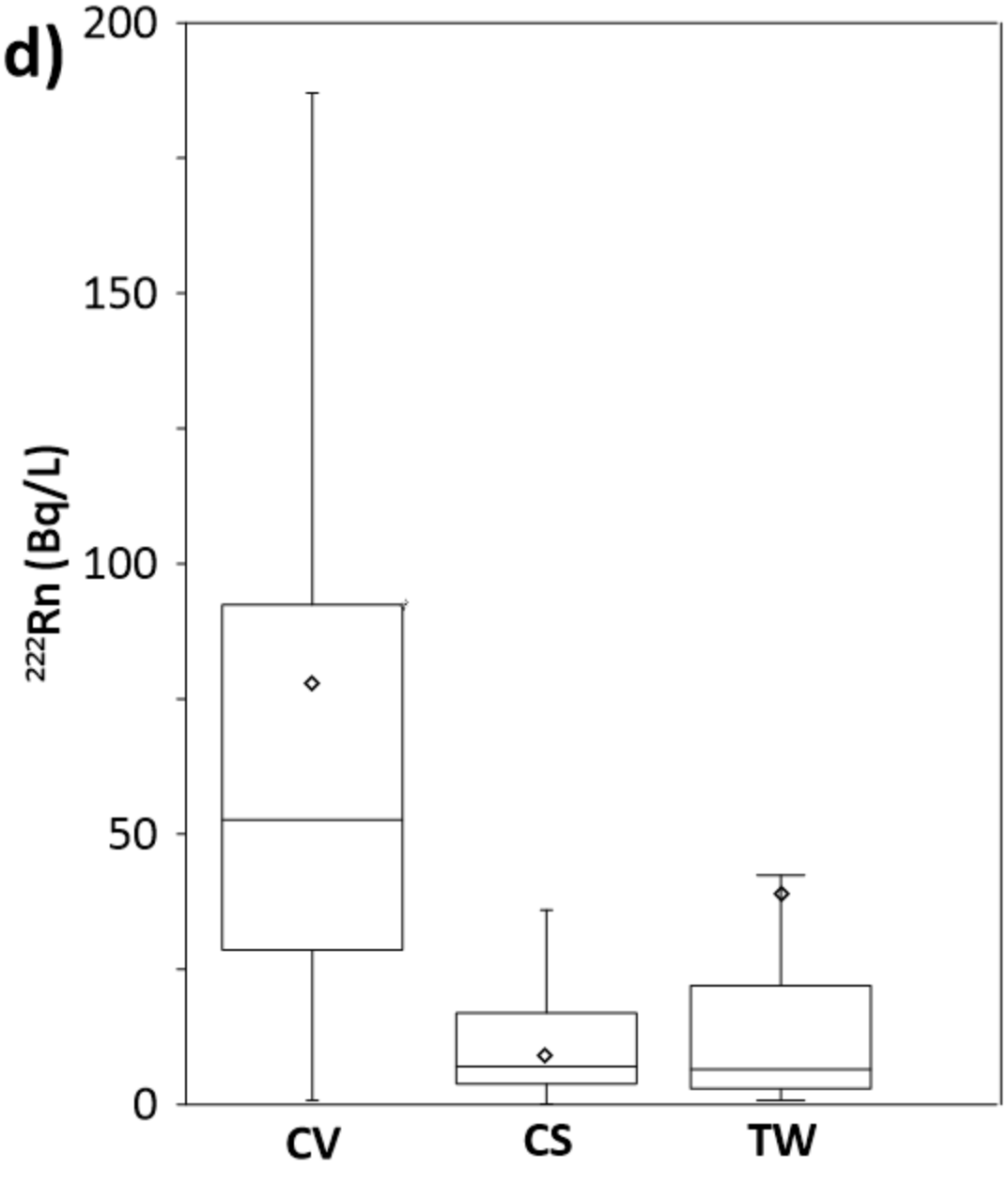
222Rn (Bq/L)
200
150
100
50
0
CV
CS
TW

N

TUSCANIA

VITERBO

ORTE

VETRALLA

Vico Lake

NEPI

TOLFA

FIANO

MANZIANA

Bracciano Lake

CIVITAVECCHIA

ANGUILLARA

Tevere River

TYRRHENIAN SEA

0 5 10 20 Km

Estimation As (µg/L)

- < 5
- 5.01 - 10
- 10.1 - 20
- 20.1 - 60
- > 60
- \+ sampling points
- alluvial deposits
- sedimentary rocks
- travertines
- volcanic rocks

N

TUSCANIA

VITERBO

ORTE

VETRALLA

Vico Lake

NEPI

TOLFA

FIANO

Bracciano Lake

CIVITAVECCHIA

ANGUILLARA

Tevere River

TYRRHENIAN SEA

0 5 10 20 Km

Estimation F (mg/L)

- < 0.5
- 0.5 - 1.5
- 1.5 - 2.5
- 2.5 - 4
- > 4
- sampling points
- alluvial deposits
- sedimentary rocks
- travertines
- volcanic rocks

N

TUSCANIA

VITERBO

ORTE

VETRALLA

Vico Lake

NEPI

TOLFA

FIANO

Bracciano Lake

CIVITAVECCHIA

ANGUILLARA

Tevere River

TYRRHENIAN SEA

0 5 10 20 Km

Estimation Rn (Bq/L)

- < 50
- 51 - 100
- 101 - 150
- 151 - 200
- > 200
- sampling points
- alluvial deposits
- sedimentary rocks
- travertines
- volcanic rocks

N

TUSCANIA
VITERBO
Cimini
VASANELLO
ORTE
VETRALLA
Vico Lake
NEPI
FALERIA
BASSANO
MONTEROSI
TOLFA
FIANO
MAGLIANO
CAMPAGNANO
MANZIANA
Bracciano Lake
CIVITAVECCHIA
ANGUILLARA
Tevere River
ISOLA FARNESE
TYRRHENIAN SEA

0 5 10 20 Km

Estimation QI

- QI=1: very low, low
- QI=2: low-to-medium, medium-to-low
- QI=3: medium, medium-to-high
- QI=4: high, very high
- sampling points
- alluvial deposits
- sedimentary rocks
- travertines
- volcanic rocks
- city limits of Rome

N

TUSCANIA

VITERBO

Cimini

FORTE

Tolfa

Vico Lake

Bracciano Lake

ANGUILLARA

CIVITAVECCHIA

Ceriti

NEPI

FIANO

Tevere River

TYRRHENIAN SEA

0 5 10 20 Km

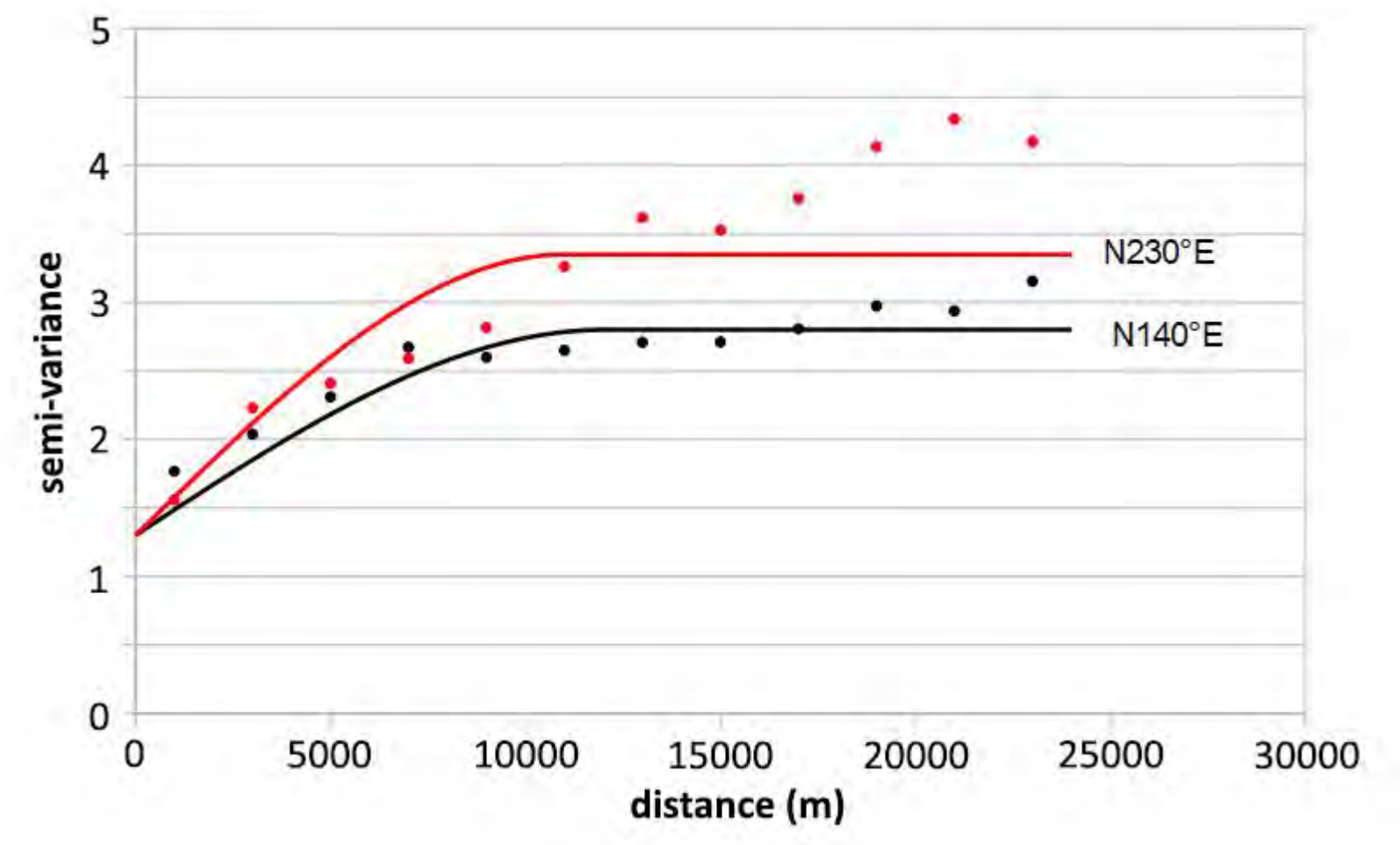
semi-variance
distance (m)
N230°E
N140°E
0
1
2
3
4
5
0
5000
10000
15000
20000
25000
30000

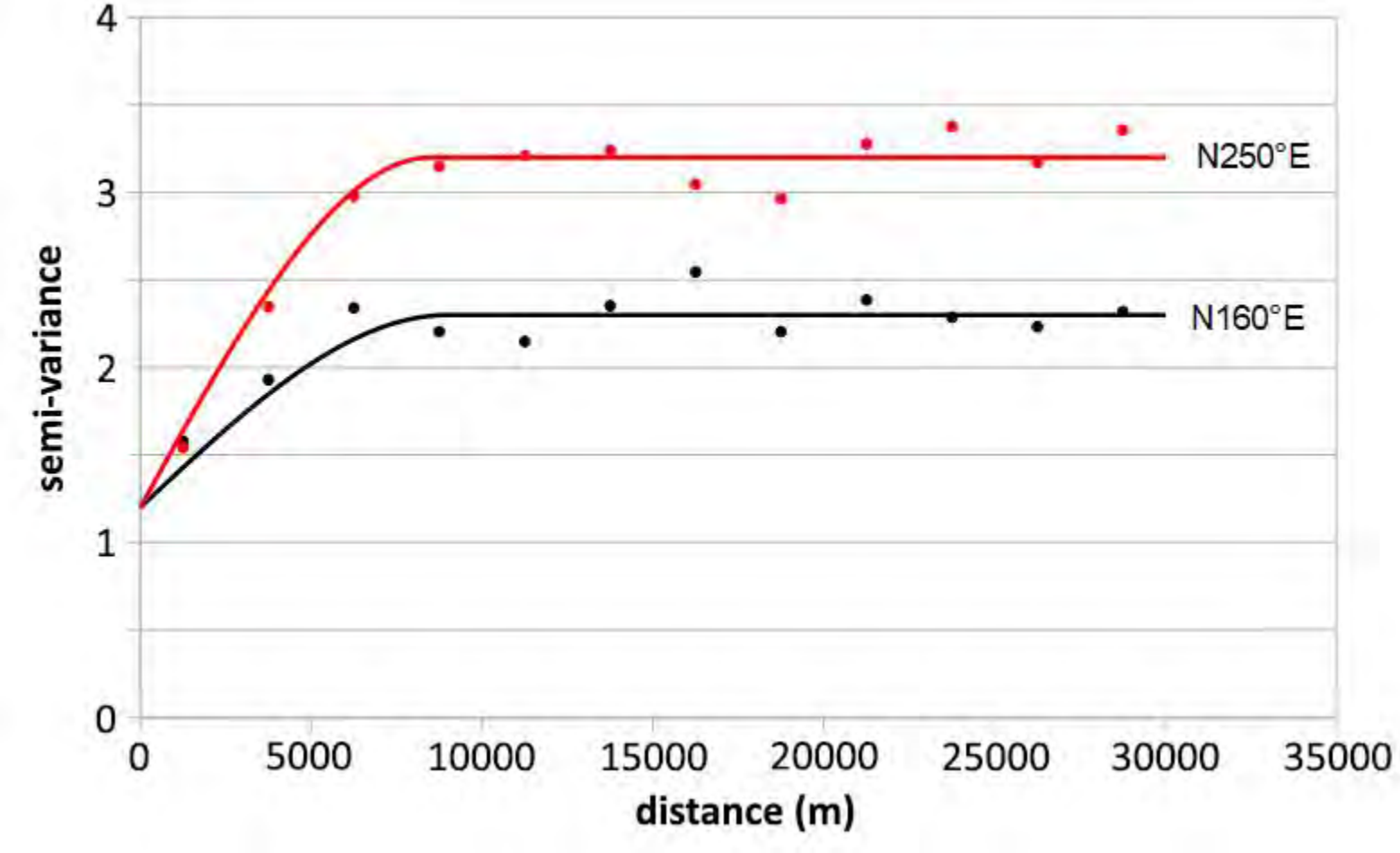
4
3
2
1
0
semi-variance
0
5000
10000
15000
20000
25000
30000
35000
distance (m)
N250°E
N160°E

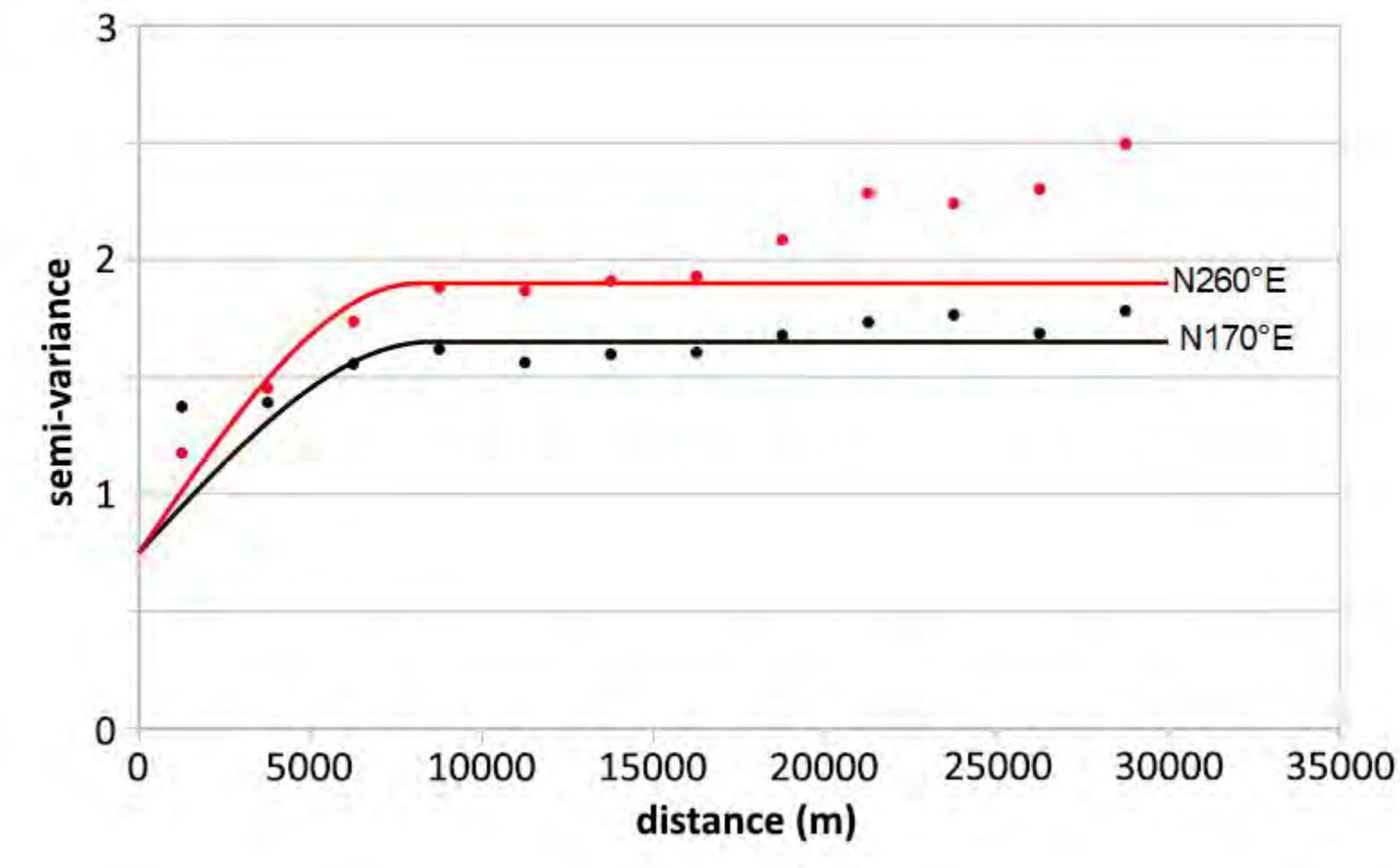
3
2
1
0
semi-variance
0
5000
10000
15000
20000
25000
30000
35000
distance (m)
N260°E
N170°E

Table 1

Arsenic	No. of observations	Min.	Max.	Q1	Median	Q3	Inter-quartile range	Average	Std-dev.	Skewness	Kurtosis
Whole population	658	0.01	1514	3.78	10.6	23.2	19.5	39.4	115	6.53	58.1
Cold-volcanic	458	0.07	296	6.01	13.2	24.3	18.3	20.4	28.8	5.54	43.0
Cold-sedimentary	127	0.01	17.6	0.36	1.06	4.28	3.93	2.67	3.31	1.71	3.02
Thermal waters	73	0.01	1514	15.8	77.3	337	321	223	278	1.98	5.60
Fluoride	No. of observations	Min.	Max.	Q1	Median	Q3	Inter-quartile range	Average	Std-dev.	Skewness	Kurtosis
Whole population	658	0.01	16.5	0.23	0.68	1.57	1.34	1.09	1.33	4.44	38.8
Cold-volcanic	458	0.01	16.5	0.27	0.72	1.48	1.21	1.09	1.38	5.20	44.3
Cold-sedimentary	127	0.01	3.81	0.11	0.23	0.55	0.44	0.43	0.62	3.62	14.9
Thermal waters	73	0.09	8.65	1.65	2.15	2.99	1.34	2.19	1.21	1.82	9.47
Radon	No. of observations	Min.	Max.	Q1	Median	Q3	Inter-quartile range	Average	Std-dev.	Skewness	Kurtosis
Whole population	640	0.10	797	10.9	36.9	76.4	65.4	60.5	82.3	3.77	21.2
Cold-volcanic	446	0.77	797	30.0	54.0	93.4	63.4	78.2	85.1	3.37	17.1
Cold-sedimentary	123	0.54	44	3.88	6.37	12.8	8.91	9.11	8.06	1.88	4.53
Thermal waters	71	0.10	698	3.02	9.11	34.5	31.5	38.7	92.5	5.54	35.4

Table 2

Element	Concentration range	QI_x	Notes
Arsenic	0 – 10	5	good quality
	10.1 – 20	3	poor quality, slightly above law limits, remediation is generally simple and cheap
	20.1 – 50	2	poor quality, above law limits, remediation is generally more complex
	> 50	1	bad quality, well above law limits, remediation is very complex and expansive
Fluoride	0 – 0.49	40	good quality, but concentration below law limits
	0.50 – 1.5	50	good quality
	1.51 – 3	30	poor quality, slightly above law limits, remediation is generally simple and cheap
	> 3	20	poor quality, above law limits, remediation is generally more complex
Radon	0 – 100	500	good quality
	101 – 200	300	poor quality, slightly above recommended limits, remediation is generally simple and cheap
	> 200	200	poor quality, above recommended limits, remediation is generally more complex

Table 3

QI	QI_x	Notes
1a	$QI_{As} = 1$, $QI_F \leq 30$, $QI_{Rn} \leq 300$	very low quality
1b	$QI_{As} = 1$, $QI_F \leq 30$, $QI_{Rn} = 500$	very low quality
1c	$QI_{As} = 1$, $QI_F \geq 40$, $QI_{Rn} \leq 300$	low quality
1d	$QI_{As} = 1$, $QI_F \geq 40$, $QI_{Rn} = 500$	low quality
2a	$QI_{As} = 2$, $QI_F \leq 30$, $QI_{Rn} \leq 300$	low-to-medium quality
2b	$QI_{As} = 2$, $QI_F \leq 30$, $QI_{Rn} = 500$	low-to-medium quality
2c	$QI_{As} = 2$, $QI_F \geq 40$, $QI_{Rn} \leq 300$	medium-to-low quality
2d	$QI_{As} = 2$, $QI_F \geq 40$, $QI_{Rn} = 500$	medium-to-low quality
3a	$QI_{As} = 3$, $QI_F \leq 30$, $QI_{Rn} \leq 300$	medium quality
3b	$QI_{As} = 3$, $QI_F \leq 30$, $QI_{Rn} = 500$	medium quality
3c	$QI_{As} = 3$, $QI_F \geq 40$, $QI_{Rn} \leq 300$	medium-to-high quality
3d	$QI_{As} = 3$, $QI_F \geq 40$, $QI_{Rn} = 500$	medium-to-high quality
4a	$QI_{As} = 5$, $QI_F \leq 30$, $QI_{Rn} = 500$	high quality
4b	$QI_{As} = 5$, $QI_F \geq 40$, $QI_{Rn} \leq 300$	high quality
4c	$QI_{As} = 5$, $QI_F = 40$, $QI_{Rn} = 500$	high quality
4d	$QI_{As} = 5$, $QI_F = 50$, $QI_{Rn} = 500$	very high quality

Supplementary Material 1

ID	Site	Type	X	Y	Aquifer	As	F^-	^{222}Rn
1	Precilia	s	263653	4669167	CV	6.0	0.21	165
2	villa Palombaro	s	263512	4669797	CV	6.9	0.60	47
3	via Oriolese	s	262958	4669166	CV	1.5	0.10	33
4	Sassone	s	261976	4669371	CV	1.8	0.05	45
5	Quadroni	s	262011	4668913	CV	2.8	0.23	94
6	Madonna delle Grazie	w	262515	4667267	CV	0.54	0.14	224
7	ponte Mariano	w	261263	4665339	CV	11	0.73	155
8	ponte Mariano	w	261016	4664240	CV	33	2.4	42
9	Madonna di Loreto	w	262601	4667553	CV	2.8	1.4	201
10	le grazie	w	263147	4667510	CV	3.0	0.31	107
11	Villa Matteini	w	263554	4668018	CV	1.7	0.67	49
12	caldara Manziana	p	260261	4664083	TW	16	1.8	n.d.
13	quarto della caldara	s	259615	4663468	CV	8.9	1.1	67
14	Aurelia-Braccianese	w	259568	4664493	CV	11	1.1	101
15	le ferriere	s	258179	4664668	CV	16	1.9	76
16	Condottino	w	258815	4663867	CV	3.6	0.30	134
17	sorgente ferruginosa	s	256569	4664625	CV	27	1.7	45
18	fontanile dell'imbastaro	s	255774	4664205	CS	n.d.	n.d.	11
19	Prata	w	261106	4670930	CV	6.8	0.99	146
20	lavatoio	s	260585	4669363	CV	5.4	0.17	64
21	Castel Donato	s	261600	4670372	CV	0.61	0.03	59
22	Casa Merenda	w	259689	4669218	CV	6.9	0.29	190
23	parco di Diosilla	p	259157	4668846	TW	9.5	8.6	25
24	fonte del Rafanello	s	257438	4668961	CS	0.80	0.68	5
25	fontanile della Bandita	s	258083	4671166	CS	0.18	0.10	3
26	fonte del Castagno	s	256782	4669608	CV	3.0	0.15	76
27	S. Fiora	w	264776	4670199	CV	9.2	0.62	106
28	sorgente del Minciaro	s	264781	4667632	CV	11	0.99	n.d.
29	ponton della mola	w	259557	4665827	CV	18	2.0	n.d.
30	prati di canale	w	257782	4666695	CV	22	2.2	86
31	quarto grande	w	257399	4666376	CV	3.8	0.05	n.d.
32	acqua di Tito	s	257484	4667107	CV	5.2	1.5	69
33	piana di Stigliano	p	254612	4667713	TW	6.7	0.95	6
34	piana di Stigliano	p	254174	4667682	TW	2.9	1.2	4
35	Terme Stigliano	s	255282	4666995	TW	1514	2.4	0.1
36	Terme Stigliano	s	255449	4667098	TW	662	2.2	4
37	Terme Stigliano	s	255451	4666999	TW	1094	2.0	3
38	Rota	s	253233	4670520	CS	5.6	1.1	9
39	Monte seccareccio	p	254818	4669580	TW	221	2.1	2
40	casale acquadoro	w	256856	4662138	TW	542	2.2	22
41	Bagnarello	s	248343	4668969	TW	149	1.9	37
42	sorgente Limoiola	s	246971	4671953	CV	18	0.04	42
43	sorgente Canale	s	247546	4671821	CV	8.9	0.04	53
44	sorgente Lizera	s	246734	4671050	CV	14	0.06	50
45	sorgente della Nocchia	s	250162	4667046	CS	0.22	0.01	8
46	strada S. Severa	s	250384	4666446	CS	0.18	0.01	4
47	Monte seccareccio	p	254639	4669724	CS	8.8	1.3	4
48	quarto della caldara	w	259749	4664228	CV	3.2	0.05	77
49	via delle fontanelle	w	259300	4665717	CV	6.7	0.56	222
50	S. Maria la Sughera	w	246194	4671288	CV	165	0.12	82
51	Concia	w	246611	4672177	CV	67	0.18	10
52	sorgente del Cerrobuco	s	249574	4667710	CS	5.1	0.07	9
53	pantanelle	s	249927	4665230	CS	0.41	0.01	4
54	monte castagno	s	251079	4667423	CS	0.37	0.01	6
55	cesi della vaccareccia	w	241275	4670091	TW	0.66	0.46	2
56	sorgente del Giglio	s	246069	4667444	CV	3.9	0.04	66
57	sorgente Fontanaccio	s	246383	4667171	CV	34	0.08	28
58	Pontonaccio	s	243065	4667864	CS	4.2	0.14	4
59	Maggiorana	w	242338	4665703	TW	2.7	0.80	1
60	poggio della stella	w	244515	4668900	CS	0.48	0.62	4
61	fontana La Bianca	w	244606	4671025	CV	1.8	0.11	62
62	fontana del Connutto	s	243814	4674209	CV	18	0.03	40
63	acqua acetosa	w	243402	4675218	CV	9.0	1.3	1
64	poggio selcioso	w	245776	4668075	TW	0.89	0.48	19
65	fontanile granciare	s	247226	4667481	CS	0.56	0.01	13
66	colle di mezzo	w	244773	4667088	CS	0.99	0.23	3
67	fontanile porcareccia	s	243415	4671244	CS	0.96	0.01	15
68	fontanile lappoleta	s	243412	4669925	TW	7.7	0.09	n.d.
69	poggio pinese	w	243972	4673354	CV	54	0.04	264

SM 1 (continued)

ID	Site	Type	X	Y	Aquifer	As	F^-	^{222}Rn
70	campaccio	w	243619	4674698	CV	115	1.3	149
71	terme ficoncella	w	237884	4668091	TW	51	1.7	2
72	fontana dell'olmo	s	253164	4663571	CS	0.48	0.07	3
73	fontana delle cannucce	s	254286	4663495	CS	0.60	0.01	3
74	valle giuncosa	s	252423	4667084	CS	0.30	0.08	6
75	fontana capannone	s	255210	4666009	CV	52	0.03	n.d.
76	fontana guarente	s	247745	4672212	CS	6.0	0.04	5
77	pian cisterna	w	250978	4672527	CV	13	0.01	92
78	poggio casalavio	s	247506	4673375	CV	19	0.14	39
79	Piana dei bagni	w	238052	4666964	TW	14	1.6	4
80	miniera	s	242280	4669189	CS	1.2	0.21	n.d.
81	fontanile le catenare	s	251645	4664591	CS	0.50	0.01	n.d.
82	borgo pantano	w	232316	4671249	TW	22	1.7	1
83	borgo pantano	w	232271	4671042	TW	28	1.7	1
84	borgo pantano	w	232778	4671234	TW	24	1.6	3
85	la frasca	w	231459	4671841	CS	2.5	0.01	19
86	la frasca	w	231365	4671326	CS	1.8	0.54	2
87	la frasca	w	231387	4671205	TW	5.5	0.46	13
88	campaccetto	w	245874	4673971	CV	2.0	0.63	52
89	monte Rovello	w	242880	4674602	CV	65	0.23	5
90	Campo di Marte	w	237196	4675657	CV	108	0.28	26
91	Campo di Marte	w	239461	4678854	CS	2.2	0.54	2
92	Bagno penale	w	234359	4666158	CS	3.4	0.08	20
93	borgo pantano	w	232171	4671019	TW	28	2.0	2
94	borgo pantano	w	232468	4671127	TW	26	1.7	3
95	fontana Pocopane	s	240180	4671601	CS	0.55	0.01	1
96	colle Tramontana	w	240827	4668648	CS	8.6	0.53	8
97	Casale dei Frati	w	248198	4670627	CS	2.4	0.19	13
98	Dolomiti del Lazio	w	252074	4660588	TW	625	1.7	17
99	borgo pantano	w	231672	4672665	CS	1.1	0.13	16
100	Pian Cisterna	w	249966	4672578	CS	0.66	3.3	8
101	caldara Vejano	w	261708	4678342	CV	1.1	0.67	30
102	font. Streppaie	s	262115	4678388	CV	12	1.0	43
103	acqua forte	s	261458	4678374	CV	1.0	0.54	229
104	fontanile sodi	s	259673	4677597	CV	13	0.27	46
105	vigna grande	s	259882	4677359	CV	13	0.26	11
106	S. Orsio	s	260305	4677901	CV	9.7	0.23	18
107	fontanile serrale	s	262292	4672267	CV	1.1	0.08	52
108	parco della mola	p	260026	4672958	TW	2.9	0.63	27
109	parco della mola	s	260030	4672910	CV	22	0.76	127
110	monte gennaro	s	260787	4677442	CV	31	0.70	6
111	le pantane	s	261792	4680016	CV	4.8	0.10	49
112	monte casella	s	258114	4676271	CS	2.7	0.06	4
113	pastinello	w	258927	4678231	CS	0.39	0.44	11
114	gorgoglione	w	260023	4679631	CV	9.2	0.36	85
115	caldara Vejano	p	261752	4678368	CV	0.23	0.28	29
116	fontanile pascolaro	s	261677	4673507	CV	6.0	0.04	23
117	fontanile cacapece	s	262565	4674562	CV	2.0	0.11	112
118	fontanile piscinello	s	263177	4674852	CV	2.0	0.07	12
119	parco della mola	s	260069	4672936	CV	2.9	0.44	249
120	civitella di cesi	s	254041	4678565	CV	11	0.34	9
121	fontanile delle 3 vasche	s	254152	4678001	CV	15	0.53	3
122	fontanile di cammerata	s	252830	4678314	CS	0.41	0.18	8
123	fontanile vaccarecce	s	253573	4676511	CS	0.26	0.01	7
124	fontanile lontaneto	s	253792	4678969	CV	18	0.86	31
125	pontone della sorca	w	252353	4674967	CS	0.50	0.13	4
126	casale vacchereccia	w	255201	4673719	CS	6.0	0.20	4
127	valle campane	w	259835	4675984	CS	0.13	0.24	13
128	monte solferata	p	255001	4657544	CV	29	17	4
129	fontanile fumarolo	s	256476	4661687	CV	9.4	0.17	77
130	fontanile sasso	s	255592	4660140	CV	8.8	0.06	82
131	villa d'Este	w	261396	4676754	CV	5.5	0.24	71
132	pian della carlotta	w	252260	4660179	TW	625	1.4	11
133	casaletto	w	263565	4672825	CV	3.2	0.30	19
134	strada della fontanella	w	263844	4673577	CV	2.7	0.14	153
135	montevirginio	w	263213	4670486	CV	5.1	0.12	41
136	poggio del fattore	w	248704	4682505	CS	3.6	0.01	5
137	poggio saracino	w	248805	4683090	CS	2.6	0.01	3
138	acqua acetosa	s	247282	4681121	CS	1.4	0.01	5

SM 1 (continued)

ID	Site	Type	X	Y	Aquifer	As	F^-	^{222}Rn
139	fontana murata	s	247945	4682460	CS	1.1	0.11	17
140	fontana della vergine	s	251174	4681191	CV	0.68	0.12	43
141	fontana del sambuco	s	250696	4680122	CV	18	1.1	95
142	fontana la casentile	s	250372	4681624	CV	12	0.27	43
143	fontana dei trocchi	s	253778	4682887	CS	0.71	0.17	44
144	santo ianni	w	263265	4673771	CV	0.98	0.13	6
145	prataline	w	261724	4676903	CV	13	0.47	35
146	le pantane	w	260609	4678142	CV	4.7	0.73	52
147	valle noce	w	262122	4676845	CV	5.4	0.16	32
148	castellina	w	263598	4674366	CV	2.5	0.06	24
149	ponte striglia	w	263296	4673955	CV	6.1	0.11	40
150	via lazio	w	263920	4672349	CV	1.9	0.10	62
151	acqua ferrata	s	254462	4659864	CV	45	0.51	44
152	le farfalle	w	265246	4664241	CV	17	1.6	56
153	lago bracciano	s	266892	4666198	CV	3.6	1.4	8
154	la lega	w	267243	4661322	CV	24	2.0	77
155	fonticiano	s	266509	4657130	CV	18	4.2	80
156	pisciarelli	w	264611	4666576	CV	11	0.49	99
157	cisterna	s	266073	4666019	CV	7.9	0.72	352
158	ponte nuovo	s	266315	4667525	CV	3.8	0.36	42
159	i terzi	s	266675	4654965	CV	14	1.3	28
160	acqua acetosa	s	267036	4655570	CV	23	0.91	60
161	monte piantangeli	s	249101	4673844	CV	4.5	0.03	57
162	fontanile cerreta	s	247771	4677119	CV	3.0	0.07	61
163	farnesiana	w	242842	4676804	CS	0.63	0.08	11
164	stazione allumiere	s	242550	4677185	CS	0.51	0.48	17
165	acqua agra	s	243179	4677389	CS	2.3	0.38	n.d.
166	fontana spinare	s	267788	4657053	CV	15	1.1	131
167	grotte civitella	w	269889	4658435	CV	59	4.8	75
168	vigna di valle	w	268496	4662205	CV	4.8	0.28	18
169	fontanile dell'aspro	s	266363	4659687	CV	8.2	0.40	6
170	fontanile della mola	s	261752	4660373	CV	12	0.80	6
171	acqua acetosa	s	261859	4662967	CV	48	1.1	27
172	trefogliette	w	261192	4664644	CV	1.1	0.39	163
173	monte bischero	s	253382	4658025	CV	259	0.58	11
174	bocca roncone	w	265712	4662673	CV	16	1.4	88
175	riserva Baccalà	w	260362	4661562	CV	13	1.5	33
176	cascata C. Giuliano	s	261905	4660154	CV	27	5.1	95
177	trefogliette	s	261402	4664518	CV	1.8	0.45	18
178	fonte del riccio	s	259297	4661782	CV	3.5	0.30	185
179	mola vecchia	p	258674	4669296	CV	47	11	4
180	comprensorio s. lucia	s	239244	4671174	CS	18	0.01	1
181	comprensorio s. lucia	w	237753	4670760	CS	12	0.34	2
182	comprensorio s. lucia	w	238026	4670533	CS	11	0.26	4
183	allumiere	w	242887	4666500	CS	0.80	3.1	2
184	monte mignolo	w	261135	4677019	CS	0.16	0.59	4
185	fontanile cerreta	s	265256	4671781	CV	5.5	0.23	55
186	crocetta	w	265712	4673015	CV	1.1	0.05	40
187	fontanile cerro	s	272575	4672591	CV	1.9	0.21	131
188	voltarina	w	263946	4667068	CV	1.2	0.68	11
189	valloni	w	265899	4674132	CV	0.07	0.17	159
190	acquaranda	w	275492	4669824	CV	27	1.3	83
191	mola vecchia	s	275645	4663340	CV	24	3.4	19
192	fontanile sogrottone	s	277208	4664146	CV	26	2.9	41
193	i due laghi	w	275839	4664596	CV	8.3	1.3	67
194	trevignano	w	272781	4670877	TW	645	2.2	32
195	longarina	w	277046	4665274	CV	30	3.3	62
196	melazza	w	280850	4663815	CV	39	2.5	20
197	procoio	w	280368	4666809	CV	2.2	0.46	36
198	valle di baccano	w	280614	4666878	TW	56	2.0	67
199	pantane	w	273411	4671535	CV	4.0	1.3	38
200	polline	w	277269	4668178	CV	14	2.4	40
201	stracciacappa	w	278795	4668311	CV	18	2.4	29
202	lagusiello	w	276101	4670652	CV	20	0.62	119
203	bagni di vicarello	s	269296	4671798	TW	34	2.1	40
204	monte del mastro	w	274752	4673349	CV	3.2	0.68	45
205	vigna grande	w	266330	4668816	CV	30	1.6	282
206	ponte formelluzzo	w	276227	4663449	CV	10	1.1	509
207	la rena	w	270622	4671193	CV	2.6	0.39	77

SM 1 (continued)

ID	Site	Type	X	Y	Aquifer	As	F^-	^{222}Rn
208	la rena	w	270223	4671186	CV	0.47	0.58	13
209	sorti lunghi	w	273058	4660012	CV	16	0.67	48
210	sorti lunghi	w	273127	4660139	CV	15	0.83	115
211	possessione	w	275208	4669386	CV	5.8	0.58	25
212	acqua claudia	w	276669	4660721	CV	8.5	0.41	26
213	martignano	w	278710	4666706	CV	69	3.8	20
214	vigna campana	w	267422	4670503	CV	37	2.5	373
215	vigna di valle	w	271294	4662173	CV	22	0.18	84
216	ginestreto	w	275407	4666425	CV	7.8	1.6	139
217	celsino	w	270393	4672359	CV	37	2.5	248
218	matiera	w	288187	4664907	CV	19	1.7	59
219	trevignano	w	272878	4670953	TW	642	2.8	268
220	acqua claudia	s	276914	4660634	TW	20	1.1	60
221	santa maria bona	s	283765	4667691	CV	6.1	1.1	11
222	fontanile papa leone	s	277266	4675850	CV	3.3	0.35	31
223	vallescura	w	279367	4681579	CV	9.0	0.96	99
224	monte lucchetti	w	277573	4674929	CV	9.2	0.56	146
225	pascolaro	w	276554	4673110	CV	13	1.2	54
226	montorso	w	288070	4677469	CV	8.1	0.43	21
227	banditaccia	w	288290	4678643	CV	12	2.0	30
228	fontanile dei coci	s	290285	4679271	CS	5.8	0.26	3
229	fontanile ruinasse	s	287001	4671479	CV	17	1.0	47
230	merlano	w	289020	4665329	CV	13	1.1	42
231	fonte levinosa	s	286856	4674285	CV	3.3	0.37	19
232	acqua rossa	s	286692	4677004	CS	0.05	3.8	6
233	fontanile dei conti	s	286821	4679005	CV	5.8	0.59	22
234	monte caio	s	283034	4674215	CV	20	0.70	70
235	fonte virgilio	s	283618	4674395	CV	20	0.68	56
236	isola dell'orso	s	283660	4673993	CV	28	0.71	92
237	fontanile botte	s	287715	4670059	CV	1.5	0.22	53
238	mortale	w	279325	4675039	CV	1.3	0.13	62
239	monte gatto	w	287795	4668141	CV	13	1.5	38
240	magliano	w	288359	4670573	CV	5.8	0.72	29
241	casale	w	290194	4677897	CV	5.1	0.30	55
242	paterno	w	288187	4681886	CV	7.1	0.30	39
243	pian paradiso	w	290613	4681687	CV	6.0	0.19	17
244	casaletti	w	290017	4676610	CV	6.4	0.32	23
245	fabbrecce	w	283060	4684022	CV	33	1.2	19
246	lavorazione marmo	w	289506	4684513	CV	13	0.80	58
247	monte s. silvestro	w	289719	4665618	CV	15	1.2	163
248	monte caminetto	w	290424	4661233	CV	31	3.6	54
249	valle scurella	w	285920	4662968	CV	14	4.0	47
250	monte le piane	w	284342	4664799	CV	62	11	81
251	sorbo	w	290815	4659088	CV	11	1.1	82
252	pian delle rose	w	282102	4672874	CV	10	0.67	70
253	monte sbucato	s	289178	4672827	CV	8.9	0.48	22
254	fontana nuova	s	286422	4665251	CV	9.2	2.4	49
255	fonte acquaviva	s	287686	4659730	CV	25	1.8	57
256	le macere	w	285363	4659044	CV	24	2.5	48
257	fonte colonna	s	293700	4666837	CV	12	0.63	29
258	fonte magnesiaca	s	292334	4667392	CV	10	0.68	112
259	fontana giglio	s	292568	4667541	CV	5.1	0.39	162
260	fonte s. antonino	s	291731	4666409	CV	11	0.69	55
261	acqua salsa	s	289738	4667120	CV	2.2	0.29	50
262	fonte vaccchereccia	s	297377	4663579	CV	15	0.97	14
263	monte sughero	w	290744	4663610	CV	9.8	1.2	29
264	monte cappelletto	w	288646	4661041	CV	17	2.2	60
265	prato della chiesa	w	288407	4666147	CV	7.3	0.76	33
266	fonte re carlo	s	285854	4654082	CV	7.7	0.26	30
267	il pino	w	284821	4653817	CS	1.3	0.23	2
268	poggio dell'ellera	w	282724	4665895	CV	20	2.4	1
269	fontana latrona	s	281850	4669721	CV	19	3.7	2
270	fonte felicia	s	295602	4665929	CS	6.2	0.39	n.d.
271	pian del cecio	w	280162	4671288	CV	14	1.8	90
272	le rughe	w	283024	4660558	CV	26	3.3	60
273	casale vaccchereccia	w	285915	4656305	TW	21	2.7	134
274	valle le piane	w	289463	4671311	CV	4.4	1.4	26
275	monte ficoreto	w	284857	4668159	CV	19	1.6	3
276	mazzangotta	w	281606	4668266	CV	0.20	4.4	75

SM 1 (continued)

ID	Site	Type	X	Y	Aquifer	As	F^-	^{222}Rn
277	roncigliano	w	284095	4672440	CV	11	0.73	46
278	s. arcangelo	w	284900	4671693	CV	13	1.8	50
279	fipestrelli	w	285928	4677326	CV	5.2	0.66	97
280	acqua acetosa	s	294574	4670162	CV	18	0.60	156
281	fontanelle	s	293712	4669697	CV	8.1	0.57	26
282	macchiano	w	285255	4666055	CV	30	3.3	33
283	monte cavone	w	288961	4661959	CV	15	1.9	43
284	villa chigi	w	285380	4660657	CV	6.0	2.3	51
285	bagni della regina	s	285709	4655469	TW	24	2.3	104
286	Giovanni XXIII	w	295037	4662580	CV	11	0.81	21
287	bastianaccio	w	293771	4663265	CV	14	0.68	13
288	quartarelle sopra	w	292969	4663928	CV	31	1.9	24
289	codette	w	292660	4660542	CV	8.0	0.87	43
290	fontana vecchia	s	296240	4666510	CV	13	1.1	17
291	quartarelle sotto	w	291765	4662240	CV	13	1.1	1
292	belvedere	w	296859	4662161	CV	24	1.8	186
293	pian dell'olmo	w	295550	4660879	CV	14	0.76	214
294	fontanile pietrò	s	291886	4668840	CV	16	0.80	11
295	p.zza del popolo	s	296520	4668633	CS	9.7	0.44	3
296	fontanile del toro	s	295859	4671806	CS	8.3	0.51	3
297	fontana cioccia	s	296788	4671513	CV	40	1.3	n.d.
298	fontanile pastinacci	s	297380	4669253	CV	1.2	0.22	92
299	fonte S. Cristina	s	298882	4666113	CS	8.7	0.46	1
300	fonte S. Marta	s	300213	4664789	CS	4.3	0.68	8
301	fonte S. Sebastiano	s	303311	4669109	CV	17	1.0	23
302	monte pereto	s	299589	4668527	CV	13	0.57	67
303	valle conca	w	298798	4669560	CV	2.4	0.41	33
304	castel campanile	s	268007	4650279	CS	1.4	3.5	3
305	fonte capo croce	s	301088	4670390	CS	1.8	0.59	10
306	fontana vecchia	s	301137	4671829	CS	1.5	0.21	18
307	sorgente pantano	s	299545	4679729	CS	1.4	0.21	5
308	madonnella	w	298543	4680941	CS	0.29	0.19	32
309	fontane nuove	w	292994	4678915	CV	19	0.57	13
310	gramiccia	w	298863	4672531	CS	2.0	0.64	17
311	val casale	w	300303	4672516	CS	0.55	0.75	30
312	sassete	w	299292	4670274	CS	3.3	1.2	15
313	fioretta	w	300387	4663831	CS	0.93	1.2	20
314	rosetoli	w	299538	4666373	CS	2.2	0.82	5
315	lavatoio del pozzo	s	296434	4668468	CV	13	0.97	6
316	fontanile primare	s	298110	4682735	CS	0.76	0.28	4
317	fonte pignatta	s	295493	4684448	CS	0.88	0.51	14
318	acqua forte	s	296090	4684859	CS	0.08	0.82	4
319	prato del cavaliere	s	296983	4683724	CS	0.12	1.2	2
320	fonte foceto	s	299410	4681696	CS	0.35	0.23	2
321	monte del re	w	289059	4653668	TW	8.5	3.0	33
322	fontanile versano	s	295146	4681508	CV	6.2	0.56	36
323	monte piccolo	s	295929	4678630	CS	9.2	0.71	6
324	pietrara	s	296153	4679319	CS	0.47	0.16	5
325	fonte dell'oncia	s	297931	4677542	CS	4.9	0.70	11
326	maiano	s	296031	4675223	CS	6.7	0.56	4
327	follonica	s	294397	4677224	CV	4.5	0.52	71
328	fonte s. agata	s	299288	4675201	CS	4.6	0.71	15
329	olgiata golf	w	282167	4658018	CV	42	6.5	49
330	cerquette	w	279699	4655293	CV	17	1.5	104
331	montelarco	w	291098	4671098	CV	17	2.0	34
332	fonte della regina	s	294045	4672954	CV	16	1.5	49
333	fonte tarabusson	s	289794	4674678	CV	5.5	1.0	13
334	fontanile pantane	s	291806	4676835	CS	6.1	0.93	7
335	monte cerasa	w	291037	4673464	CV	7.7	1.1	44
336	ospedaletto	w	286791	4651838	CS	1.9	1.2	2
337	casalino	w	278215	4670073	CV	13	2.5	139
338	vigne nuove	w	279770	4673258	CV	11	1.2	69
339	monte li servi	w	284661	4676980	CV	14	1.2	56
340	soriano	w	285859	4675397	CV	19	3.4	40
341	monte gemini	w	284628	4669769	CV	28	4.2	35
342	cesano	w	279098	4660645	CV	8.8	1.9	35
343	isola farnese	w	283750	4654886	CV	1.6	0.65	37
344	flaminia	w	291861	4656955	CV	5.9	0.92	41
345	grotta franca	w	284049	4662594	CV	6.0	3.8	3

SM 1 (continued)

ID	Site	Type	X	Y	Aquifer	As	F^-	^{222}Rn
346	castelluccia	w	284224	4651216	CV	2.8	0.67	7
347	casale acquaviva	w	280976	4652467	CV	18	0.59	5
348	fosso piordo	s	284411	4655516	TW	17	2.2	32
349	val pantana	w	290016	4655047	CV	5.5	3.4	5
350	sorgente rosciolo	s	276692	4656720	CV	34	1.9	n.d.
351	fonte malinverno	s	276340	4652285	CV	34	1.6	7
352	ara delle rose	w	288150	4657297	CV	6.4	1.2	20
353	torre chiavello	w	292729	4683762	CV	5.9	0.46	30
354	monte dell'ara	w	274200	4648992	CV	38	1.6	62
355	fontanile tragliata	s	273697	4650245	CV	73	4.1	35
356	fonte lanciafava	s	279135	4649310	CV	31	2.1	4
357	fonte della comunella	s	278631	4652694	CV	18	1.0	26
358	bocceola	w	277476	4649990	CV	6.5	0.58	11
359	colle sabazio	w	273654	4657779	CV	56	3.6	47
360	ponton dell'elce	w	271176	4656232	CV	50	3.9	54
361	quarto della torre	w	268965	4653604	CV	51	2.3	51
362	castellaccio	w	270826	4651097	CS	12	0.55	1
363	pontoni	w	272733	4653453	CV	40	2.3	68
364	S. Maria dei monti	w	267540	4677461	CS	0.19	0.29	4
365	poggio Pupugliano	w	266545	4675687	CV	0.76	0.05	180
366	fonte Casciano	s	268180	4675299	CV	1.3	0.09	94
367	fonte Ceraso	s	269744	4675227	CV	2.5	0.25	26
368	fonte Chiappini	s	267755	4673755	CV	2.9	0.57	82
369	fonte Pantano	s	264184	4675264	CV	0.91	0.13	38
370	poggio Polveroso	w	265061	4676672	CV	1.0	0.08	188
371	Agliola	w	264146	4678339	CV	0.88	0.08	101
372	Mola di Bassano	s	269648	4679192	TW	13	1.2	698
373	pian del Vescovo	p	268491	4679540	CV	0.59	1.5	47
374	fontanile S. Martino	s	275547	4676809	CV	2.2	0.17	32
375	pian della Iella	w	271014	4683417	CV	41	1.5	160
376	Sutri	w	270410	4681217	CV	16	0.46	62
377	Sercione	w	274559	4679021	CV	11	1.7	39
378	bosco Fonte	w	272296	4675455	CV	5.2	0.36	52
379	pian Giudeo	s	272156	4679339	CV	8.5	0.48	7
380	Vivola	w	272352	4680407	CV	13	1.0	102
381	fontanile Calandrina	s	270658	4673991	CV	1.9	0.29	33
382	poggio Tramontana	w	273869	4674244	CV	18	1.9	187
383	Bassano	w	268343	4678310	CV	4.5	0.09	69
384	fonte Vangata	s	255806	4680426	CV	14	0.77	12
385	fonte Sgrulla	s	256760	4679796	CS	0.11	0.10	9
386	fonte pian del Nasse	s	256826	4680943	CS	0.12	0.48	29
387	acqua Magnesia	s	257953	4682307	CV	46	0.92	29
388	Paliano	w	257797	4695977	TW	358	3.0	2
389	terme dei Papi	w	258587	4700138	TW	289	3.0	7
390	sorgente del Papa	s	258589	4700024	TW	14	2.2	53
391	Bullicame	p	259255	4700800	TW	356	3.1	4
392	pozzo Zitelle	p	258201	4701470	TW	293	3.1	3
393	sorgente Zitelle	p	258276	4701478	TW	297	3.1	3
394	piscina Carletti	p	258586	4700992	TW	336	3.2	3
395	S. Valentino	w	259357	4701458	TW	337	2.8	13
396	S. Albino	p	259260	4701522	TW	325	3.1	5
397	sorgente Garinei	p	258744	4705143	TW	215	3.1	3
398	sorgente Oasi	p	259359	4705707	TW	271	3.2	3
399	lago Bagnaccio	p	259256	4705276	TW	319	3.5	16
400	lago Bagnaccio	p	259195	4705278	TW	16	1.7	12
401	fonte acqua Rossa	s	263343	4707323	CV	17	1.8	30
402	S. Caterina	s	258438	4700124	TW	286	1.8	76
403	Bagni	s	258627	4700014	TW	611	2.8	123
404	Montarozzo	w	259333	4703840	TW	242	2.7	41
405	Montarozzo	p	259553	4703908	TW	390	3.1	11
406	Masse S. Sisto	p	257848	4695518	TW	397	3.1	4
407	Bussete	p	258708	4701785	TW	366	3.6	2
408	SMAM 1	s	259045	4702129	TW	19	2.2	8
409	SMAM 2	s	259127	4701601	TW	393	3.3	6
410	S. Cristoforo	p	258011	4698478	TW	319	3.2	11
411	Masse S. Sisto	w	258346	4695802	TW	77	2.0	113
412	S. Cristoforo	p	258042	4698407	TW	316	3.1	4
413	Madonna del Ponte	w	256284	4689172	CV	14	1.0	129
414	piazza Castello	w	287532	4692321	CV	17	0.90	11

SM 1 (continued)

ID	Site	Type	X	Y	Aquifer	As	F^-	^{222}Rn
415	lago Vico	s	269859	4688387	TW	14	0.98	1
416	S. Rocco	w	270756	4690623	CV	43	1.6	134
417	monte Venere	s	268577	4692929	CV	6.0	0.12	21
418	fontana Cavette	s	264922	4688094	CV	8.2	0.83	42
419	Magliano basso	w	271788	4689626	CV	46	1.8	48
420	fontana Pilo	s	272459	4689880	CV	14	0.35	122
421	Barco	w	275268	4685313	CV	42	1.3	175
422	sorgente Carestia	s	272465	4691017	CV	16	0.30	65
423	Casello	w	268152	4683756	CV	50	1.5	415
424	poggio Cavaliere	w	268427	4687117	TW	286	1.7	180
425	Vallonzano	w	258729	4685846	CV	19	0.96	47
426	sorgente la Vena	s	258322	4685794	CV	15	0.95	58
427	fontanile Nuovo	s	251812	4683292	CS	0.22	0.12	7
428	fontana Candida	s	277170	4697360	CV	7.6	0.14	46
429	fontana della Vita	s	264594	4692426	CV	31	0.08	90
430	fonte Orioletto	s	269764	4692324	CV	24	1.9	39
431	Passanella	w	271503	4686399	CV	17	0.22	149
432	stazione Ronciglione	w	270663	4685230	CV	14	0.75	164
433	Chianello	w	269624	4685566	CV	29	1.0	158
434	sorgente Neri	s	267925	4682013	CV	18	0.90	181
435	XXX miglia	w	275898	4681604	CV	15	0.83	56
436	campo Rotondo	w	263521	4683358	CV	18	0.99	128
437	AVES	s	259151	4701451	TW	328	2.9	36
438	AVES	p	259330	4701148	TW	373	2.9	7
439	Vasella	w	264061	4684289	CV	18	0.44	70
440	poggio dell'Ulivo	p	264846	4709781	TW	7.8	0.50	11
441	Bagnaccio	w	259016	4704694	TW	171	3.3	4
442	fontana del Boia	s	259963	4700596	TW	18	1.7	27
443	sorgente Vipera	s	260994	4680779	CS	0.37	0.12	7
444	la Chiusa	w	259330	4681587	CS	0.10	0.19	9
445	Beccacceto	w	270188	4684453	CV	25	1.1	91
446	Pozzo	w	264415	4685623	CV	13	1.8	36
447	Setano	w	258570	4689202	CV	23	1.2	74
448	Capacqua	w	258298	4691908	CV	44	0.80	81
449	Cunicchi	w	260767	4691149	CV	25	1.2	63
450	Noce	w	260589	4688940	CV	37	0.67	150
451	Grignano	s	258534	4687168	CV	20	1.1	115
452	Cinelli	w	251208	4690855	CV	32	2.7	54
453	monte Jugo	w	257442	4708907	CV	21	1.5	80
454	monte Vitorchiano	w	268283	4702229	CV	18	0.17	74
455	poggio Pasquale	w	267484	4707739	CS	4.4	0.10	6
456	sorgente Scemato	s	270200	4708107	CV	16	2.8	92
457	Mazzatosta	w	266540	4705217	CV	8.6	0.20	31
458	S. Giuseppe	w	280580	4699375	CV	6.7	0.23	33
459	Precujaro	w	265212	4680324	CV	13	0.72	76
460	sorgente Pidocchio	s	258050	4697468	CV	21	0.52	195
461	Riotrai	w	266740	4701933	TW	25	0.15	42
462	sorgente Roncone	s	264311	4697874	CV	7.4	0.21	164
463	Mensa bassa	w	263200	4699193	CV	12	0.32	127
464	fonte Settecannelle	s	264050	4701042	CV	9.6	0.21	82
465	Canale	w	262191	4693613	CV	38	0.71	103
466	Balletti	w	263164	4695226	CV	5.8	0.26	70
467	Cimina	w	267199	4697512	CV	8.4	0.13	96
468	fontana di Ronci	s	282060	4676644	CV	16	1.2	110
469	terme dei Gracchi	p	280615	4677542	CV	0.17	1.7	37
470	fontanile Venti Rubbia	s	246716	4685515	CS	0.10	0.08	20
471	fontanile Grande	s	248130	4685111	CS	0.01	0.15	4
472	fontanile S. Angelo	s	262836	4689205	CV	7.3	0.14	27
473	valle Carpineta	s	261741	4688771	CV	12	0.40	157
474	Capacqua	w	258072	4692383	CV	58	1.3	95
475	fontana piano Aiano	s	259012	4685158	CV	5.1	0.10	534
476	Acquamatta	w	253846	4701729	CV	22	1.8	24
477	Creti	w	272171	4680881	CV	4.5	0.12	51
478	Annunziatella	w	274514	4683219	CV	8.0	0.40	64
479	Vignola	w	272837	4688430	CV	33	0.94	76
480	acqua di Nepi	w	280656	4677466	CV	7.7	1.2	49
481	Montarone	w	258037	4700043	CV	296	1.7	8
482	Monterazzano	w	255669	4703288	CS	0.53	0.17	8
483	Viterbo	w	262891	4701224	CV	12	0.22	14

SM 1 (continued)

ID	Site	Type	X	Y	Aquifer	As	F^-	^{222}Rn
484	S. Salvatore	w	261522	4703599	CV	40	0.92	53
485	Tobia	w	260930	4696167	CV	23	0.76	96
486	Procoio	w	254776	4698609	CV	59	1.3	8
487	Camorelle	w	251147	4697985	CV	57	2.5	1
488	Tuscanese	w	256649	4700990	CV	60	0.95	20
489	Ficoncella	w	252217	4704384	CV	7.4	0.64	28
490	strada Romana	w	266122	4700633	CV	7.4	0.16	73
491	Nibbio	w	263890	4694080	CV	24	0.68	106
492	Monticello	w	257308	4683967	CV	5.8	0.19	60
493	macchia Nuova	w	253993	4681483	CS	0.01	0.30	13
494	Antaneto	w	261893	4684104	CV	3.9	0.19	300
495	Cerro	w	278716	4680167	CV	19	1.7	93
496	Vico Matrino	w	262862	4684774	CV	17	1.7	1
497	pian di Nero	w	264453	4702090	CV	11	0.23	11
498	Roncone	w	263909	4698651	CV	9.1	0.22	62
499	Perella	w	268751	4698879	CV	2.7	0.06	35
500	Sambuco	w	264083	4681748	CV	12	0.35	35
501	Sacrocuore	w	266464	4682768	CV	43	0.94	467
502	Varano	w	277916	4682141	CV	51	1.7	115
503	Concio	w	280485	4679433	CV	27	4.1	132
504	Galilei	w	282455	4679758	CV	57	2.4	115
505	S. Paolo	w	282074	4681203	CV	60	2.5	91
506	Pantane	w	278019	4679443	CV	18	0.09	65
507	villa Canonica	w	257800	4689141	TW	0.08	0.74	5
508	fontanile Calisto	s	246236	4683080	CS	0.07	0.16	6
509	fontana dei Giunchi	s	244550	4683301	CS	0.09	0.16	4
510	fontana Trocchetti	s	243226	4685979	CS	0.12	0.11	4
511	fontanile Catone	s	242170	4687512	CS	0.14	0.12	8
512	fontanile Pascolare	s	244749	4686246	CS	0.20	0.10	12
513	poggio acqua Fredda	w	254013	4689008	CV	37	2.4	72
514	Piombinello	w	256642	4690809	CV	16	1.2	135
515	Pompieri	w	287094	4687361	CV	50	0.85	9
516	Sassacci	w	288246	4688508	CV	16	0.42	15
517	Monticelli	w	289736	4689376	CV	37	0.82	15
518	Borghetto	w	290269	4690872	CV	19	1.3	7
519	Roccarespampani	w	247534	4697429	CV	9.0	1.2	77
520	Roccarespampani	w	249127	4699006	CV	17	3.4	21
521	sorgente Pidocchio	s	245984	4695635	CV	17	2.4	182
522	pian di Nero	w	264276	4702867	CV	6.6	0.08	38
523	valle Castellane	w	258405	4706469	CV	25	2.0	447
524	Grottone	w	268303	4697873	CV	14	0.47	797
525	Cacciabella	s	258250	4700167	CV	280	1.8	31
526	pian delle Vigne	w	250109	4691539	CV	33	2.3	87
527	Cerracchio	w	252351	4688630	CV	13	1.5	81
528	Mazzocchio	w	257708	4688088	CV	12	0.53	16
529	Botte	w	260748	4687259	CV	13	0.16	115
530	Doganella	w	253529	4691374	CV	28	1.2	6
531	Mangane	w	255429	4692461	CV	54	1.0	37
532	pian del Gentile	w	253352	4694972	CV	80	1.7	25
533	Bellomo	w	257079	4686274	CV	1.6	0.55	12
534	Falerii	w	282848	4686325	CV	43	1.9	95
535	S. Lorenzo	s	282563	4684510	CV	48	1.8	61
536	Barco	w	284004	4684387	CV	43	1.7	42
537	Cenciano	s	280076	4692681	CV	13	0.37	33
538	Forticella	w	274777	4691325	CV	23	0.92	131
539	Cesurli	w	279692	4700141	CV	8.5	0.16	79
540	Parano	w	282629	4699498	CS	3.3	0.09	4
541	Crocicchia	w	278123	4703707	CV	5.3	0.14	63
542	campo Fiera	w	278319	4704971	CS	3.5	0.11	19
543	poggio Rosso	w	278892	4704704	CS	4.2	0.16	1
544	barca di S. Francesco	w	288358	4699638	CS	0.22	0.20	43
545	Molignano	w	287513	4701369	CS	0.99	0.26	1
546	Cimacolle	w	284915	4705794	CS	0.26	0.90	2
547	Mauraccio	w	284619	4705573	CS	0.30	0.65	1
548	Cappuccini	w	282477	4703601	CS	8.6	0.55	1
549	Pontaccio	s	285320	4704893	CS	0.18	0.29	10
550	Petignano	w	285758	4705299	CS	0.14	0.43	19
551	Taccia	w	282842	4704881	CS	0.42	0.81	29
552	coste Santarelli	w	279861	4706305	CS	0.77	0.30	19

SM 1 (continued)

ID	Site	Type	X	Y	Aquifer	As	F^-	^{222}Rn
553	terme Orte	w	281983	4704245	TW	3.7	1.8	9
554	Mezzo Frate	w	285169	4693773	CS	6.0	0.65	18
555	Bandita	w	268906	4704975	CV	12	0.09	20
556	scalo Teverina	w	288792	4695319	CS	2.9	0.30	13
557	Valli	s	288146	4694642	CS	2.2	0.17	4
558	Chiare Fontane	s	279560	4695770	CV	11	0.42	54
559	Cacciarino	w	286432	4706983	CS	0.03	0.59	5
560	Piscinale	w	286641	4703955	CS	6.2	0.44	11
561	Tre Ponti	w	281723	4706217	CS	0.34	0.63	19
562	torre Amena	w	283670	4702289	CS	1.3	0.16	6
563	tenuta Bagnolo	w	285646	4699446	CS	4.4	0.18	15
564	Radicare	w	286442	4697412	CS	4.2	0.17	10
565	macchia di Ruffo	w	288248	4698830	CS	9.0	0.25	7
566	poggio Ruzzolo	w	279998	4704595	CS	5.4	0.33	11
567	poggio Capraro	w	278383	4705889	CS	4.8	0.05	18
568	S. Marco	w	283548	4701417	TW	0.01	0.27	1
569	casa Umbertini	w	282589	4694368	CS	5.5	0.44	17
570	poggio Capre	w	287255	4694062	CS	8.5	0.33	10
571	Corteccoli	w	288700	4693317	CV	14	0.62	9
572	Selvaluce	w	271570	4696084	CV	6.6	0.04	117
573	pozzo n. 3	s	269670	4695567	CV	4.7	0.09	111
574	fontana Rosa	s	271632	4694981	CV	10	0.12	166
575	Pieve	w	274077	4696437	CV	14	0.10	42
576	Vignola	w	275529	4696152	CV	14	0.20	69
577	Montecchie	p	284522	4707283	CS	10	0.25	4
578	poggio Foralupo	p	264189	4710819	CV	33	2.4	n.d.
579	acqua Forte Tuscania	s	244706	4703730	TW	16	2.4	107
580	solforata Marta	p	243698	4695095	CV	101	4.7	2
581	Selva	w	275778	4692602	CV	17	0.30	93
582	Salvani	s	276959	4690452	CV	4.7	0.47	180
583	Barco	w	277251	4690288	CV	36	0.68	159
584	Catalano	w	280449	4688337	CV	44	1.5	337
585	Rigolelli	w	281321	4685854	CV	60	1.7	349
586	Quartaccio	w	282784	4688506	CV	61	2.7	49
587	S. Lazzaro	w	244578	4699664	CV	33	1.7	10
588	S. Giusto	w	243618	4697860	CV	8.3	0.62	194
589	le Guinze	w	246494	4702123	CV	21	1.3	73
590	Tuscania	w	242020	4701307	CV	7.7	0.61	50
591	Piantacciano	w	245862	4699273	CV	20	1.2	44
592	pian dell'Olmo	w	258880	4693206	CV	112	1.9	402
593	Chia	w	276370	4704757	CV	7.5	0.10	52
594	S.Eutizio	w	275911	4700177	CV	20	0.26	84
595	Vasuccino	s	270612	4701031	CV	4.5	0.03	55
596	Acquaspasa	s	268954	4699953	CV	5.2	0.02	27
597	doppio G	w	271721	4700065	CV	8.8	0.04	171
598	Cicella	s	272630	4698682	CV	5.2	0.05	34
599	Cacciabella	w	258590	4700513	TW	516	3.2	9
600	Artete	w	278903	4692533	CV	14	0.24	50
601	selva Ferrante	w	279780	4694889	CV	19	0.31	2
602	Centignano	w	277395	4698489	CV	12	0.30	236
603	Quartuccio	w	256989	4693830	CV	56	0.95	263
604	S. Giovanni	w	256627	4691222	CV	57	0.62	180
605	stazione Corchiano	w	281572	4691936	CV	19	1.9	72
606	Vantignana	w	283033	4690242	CV	38	1.6	8
607	Bandita	w	279920	4689488	CV	26	2.2	73
608	piano di valle Cupa	w	277028	4685958	CV	55	1.3	449
609	Nicicchiola	w	266572	4692210	CV	72	1.3	29
610	Fornacchia	w	269712	4702722	CV	15	0.11	33
611	Poggiarella	w	270810	4706671	CV	4.9	0.10	28
612	Sanguetta	s	273719	4704385	CV	10	0.25	62
613	Civitelle	w	277401	4705710	CV	4.2	0.25	28
614	Crocetta	w	276769	4700798	CV	12	0.55	66
615	Sardinello	w	273678	4700351	CV	6.6	0.21	60
616	Crocifisso	s	274858	4693527	CV	4.9	0.64	131
617	Casalaccio	w	285631	4685001	CV	26	1.2	36
618	podere Giustina	s	239509	4693104	CV	4.7	0.58	88
619	podere Annina	s	240499	4691526	CV	13	1.1	11
620	S. Giusto	w	242591	4697080	CV	15	1.3	95
621	Chiusa	w	285810	4683477	CV	10	1.3	25

SM 1 (continued)

ID	Site	Type	X	Y	Aquifer	As	F^-	^{222}Rn
622	Mola	w	282920	4681644	CV	39	1.7	87
623	Umiltà	w	280367	4677053	CV	3.5	0.67	239
624	Ronci	w	281093	4676952	CV	9.3	1.4	84
625	Bandita	w	285080	4680968	CV	39	2.1	57
626	poggio S. Quirico	w	278933	4701748	CV	5.6	0.19	36
627	pontone Moricchio	w	283351	4698828	CS	1.9	0.09	4
628	Rinchiusa	w	271017	4696900	CV	9.5	0.07	113
629	poggio Cupellone	w	260621	4683093	CS	0.74	0.23	13
630	S. Andrea	w	276022	4687848	CV	77	1.5	152
631	le Pantane	w	275955	4702732	CV	7.2	0.30	89
632	lago Vadimone	s	280062	4707194	CS	1.7	0.80	n.d.
633	Ranucci	w	266572	4696940	CV	8.5	0.18	70
634	Palazzolo	w	280371	4701905	CV	4.7	0.25	37
635	Fogliano	w	265830	4690119	TW	495	2.9	102
636	Scopetone	w	259548	4706315	CV	119	1.9	41
637	S. Silvestro	w	287088	4689240	CV	29	1.2	8
638	Capannella	w	277096	4687612	CV	44	1.0	72
639	Caprini	w	262018	4704646	CV	36	0.76	123
640	Paraceneri	w	257272	4706532	CV	5.7	0.29	60
641	Cavallaccia	w	242325	4695419	CV	11	0.96	56
642	due Casali	w	260398	4696012	CV	56	1.8	140
643	Rimessa	w	247908	4689006	CS	0.36	0.20	7
644	Fornacelle	w	252632	4687178	CV	6.2	0.52	44
645	grotta Porcina	w	252588	4687557	CV	10	0.25	8
646	S. Angelo	w	272223	4701446	CV	4.9	0.11	217
647	S. Francesco	w	285390	4688049	CV	26	1.6	127
648	Borgherolo	w	250321	4694381	CV	18	0.70	31
649	Occhio di Becco	w	252076	4691700	CV	25	1.7	35
650	Mazzocchio	w	257249	4688264	CV	14	0.52	92
651	pian del Pero	w	252996	4696121	CV	28	1.9	110
652	Bicocca	w	251724	4694513	CV	39	1.0	71
653	Cinelli	w	250473	4687236	CV	9.6	1.1	42
654	Ponte Minchione	w	280260	4683925	CV	37	1.3	78
655*	Fratta	w	284154	4691428	CV	23	1.5	n.d.
656*	Botte	w	284791	4695251	CV	2.5	0.20	n.d.
657*	Loretta	w	282384	4698008	CV	4.5	0.20	n.d.
658*	S. Silvestro	w	288397	4691041	CV	16	0.80	n.d.
659*	Boschetto	w	277255	4694497	CV	15	0.30	n.d.

Supplementary Material 3

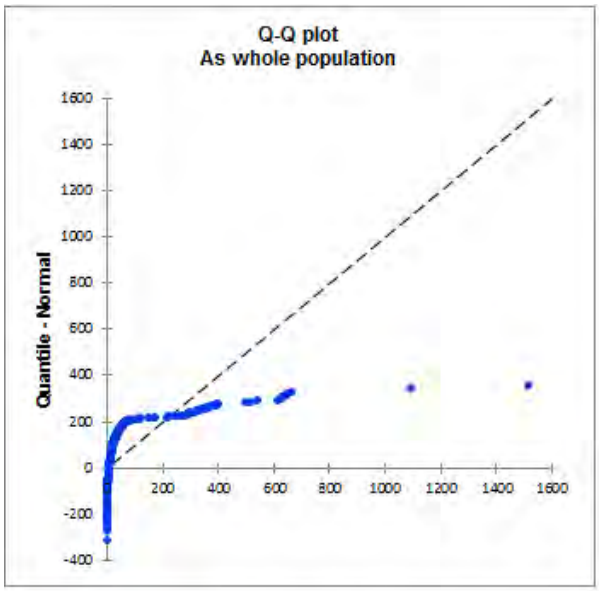

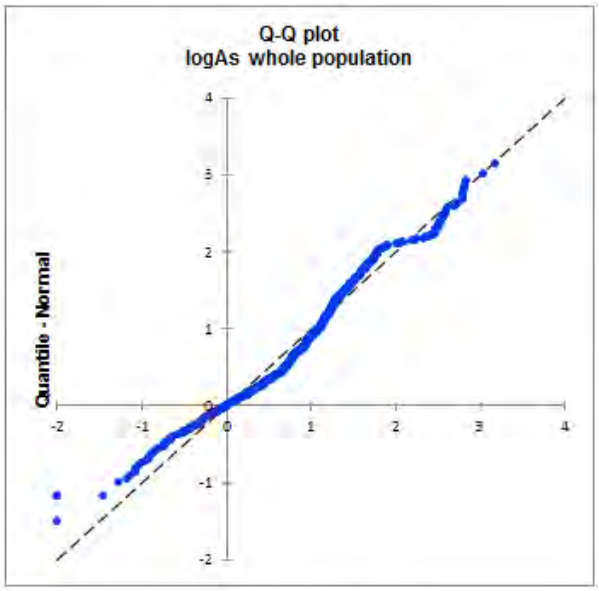

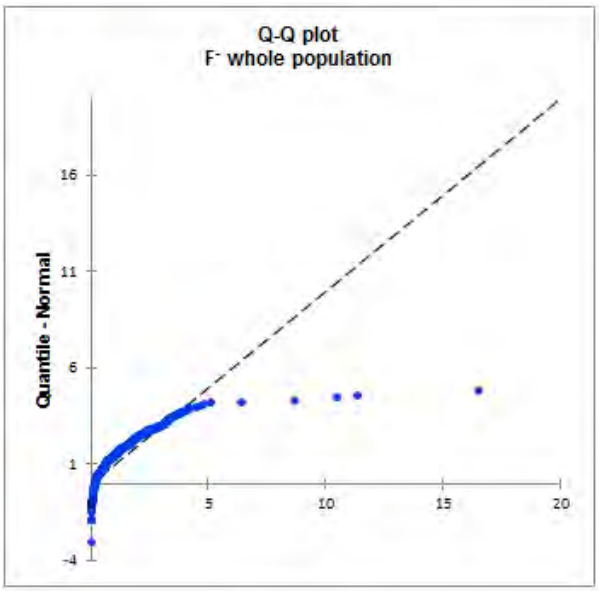

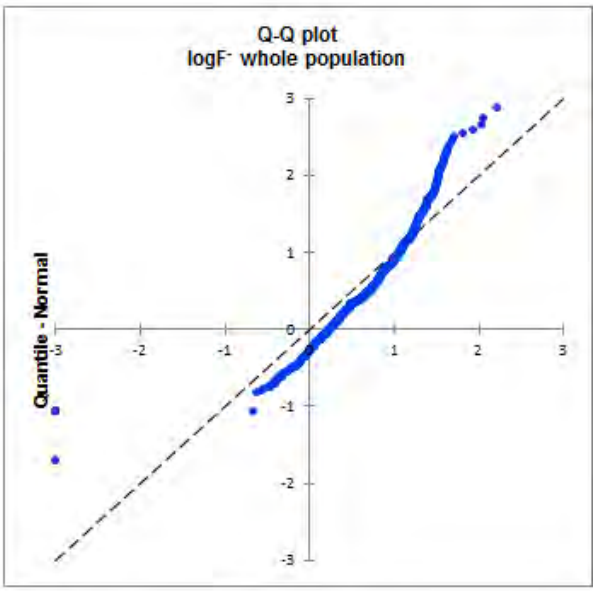

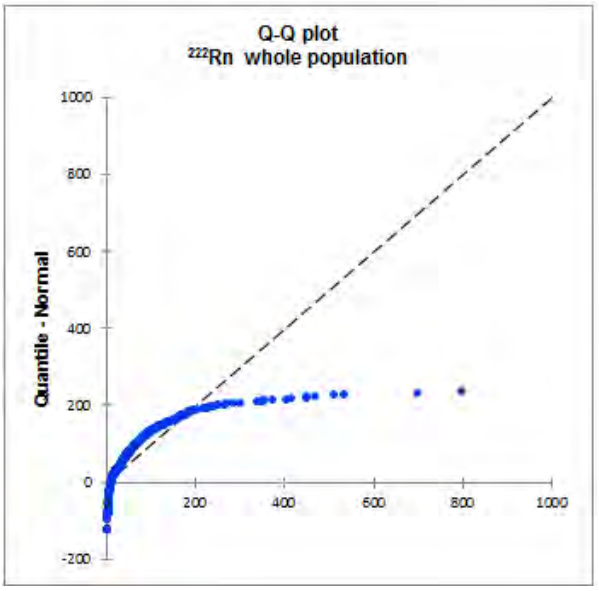

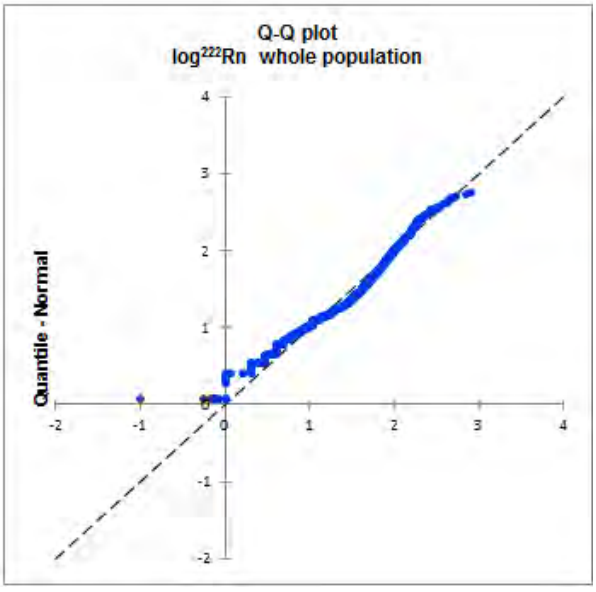

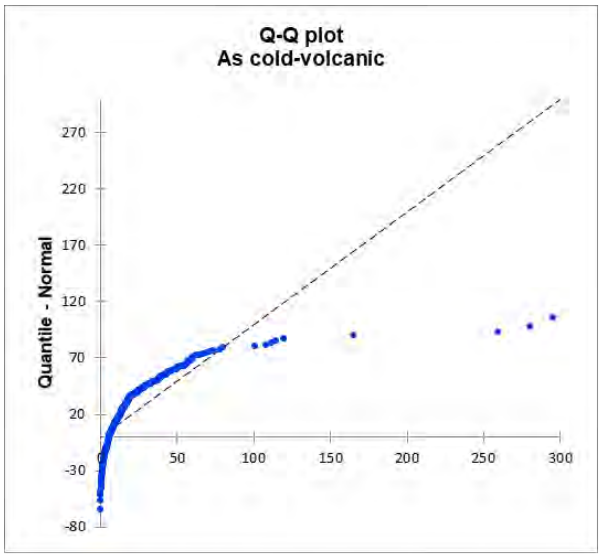
Q-Q plot
As cold-volcanic
Quantile - Normal
270
220
170
120
70
20
-30
-80
50
100
150
200
250
300

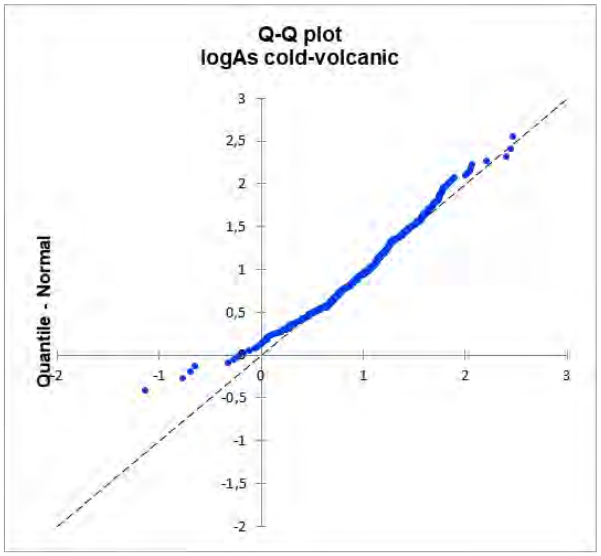
Q-Q plot
logAs cold-volcanic
Quantile - Normal
3
2,5
2
1,5
1
0,5
-0,5
-1
-1,5
-2
-2
-1
0
1
2
3

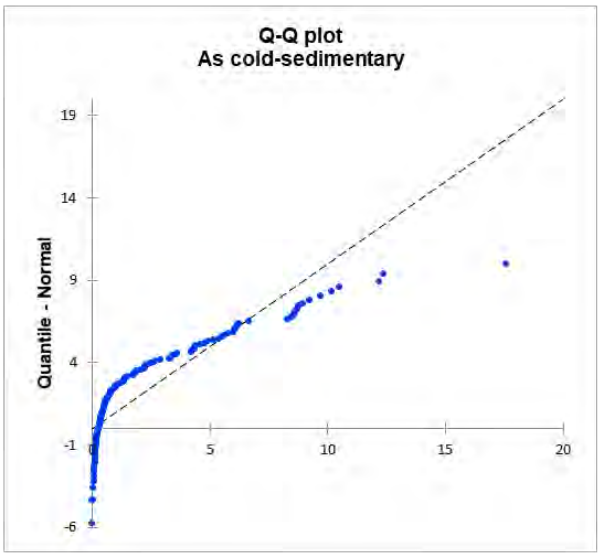
Q-Q plot
As cold-sedimentary
Quantile - Normal
19
14
9
4
-1
-6
5
10
15
20

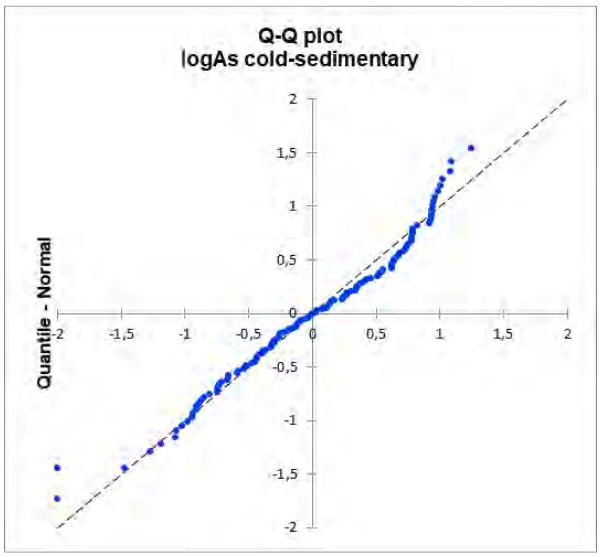
Q-Q plot
logAs cold-sedimentary
Quantile - Normal
2
1,5
1
0,5
-0,5
-1
-1,5
-2
-2
-1,5
-1
-0,5
0
0,5
1
1,5
2

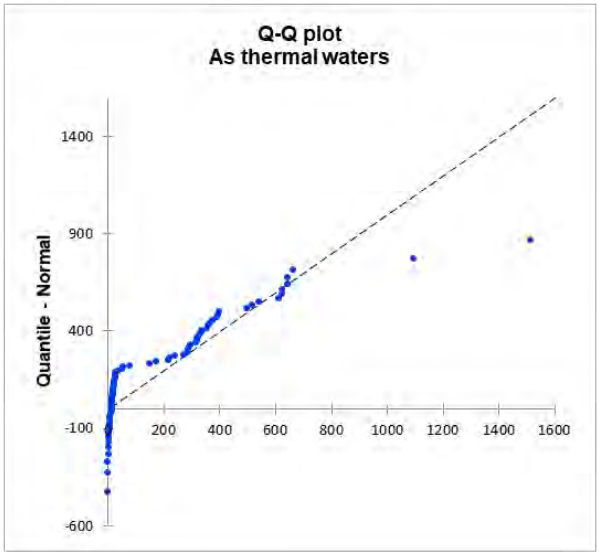
Q-Q plot
As thermal waters
Quantile - Normal
1400
900
400
-100
-600
200
400
600
800
1000
1200
1400
1600

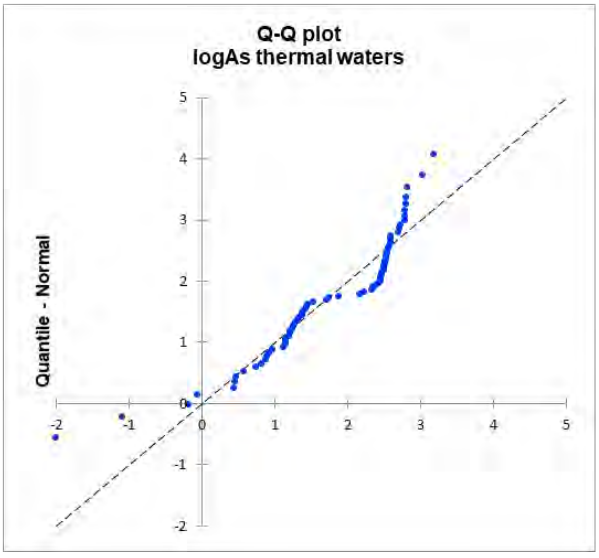
Q-Q plot
logAs thermal waters
Quantile - Normal
5
4
3
2
1
-1
-2
-2
-1
0
1
2
3
4
5

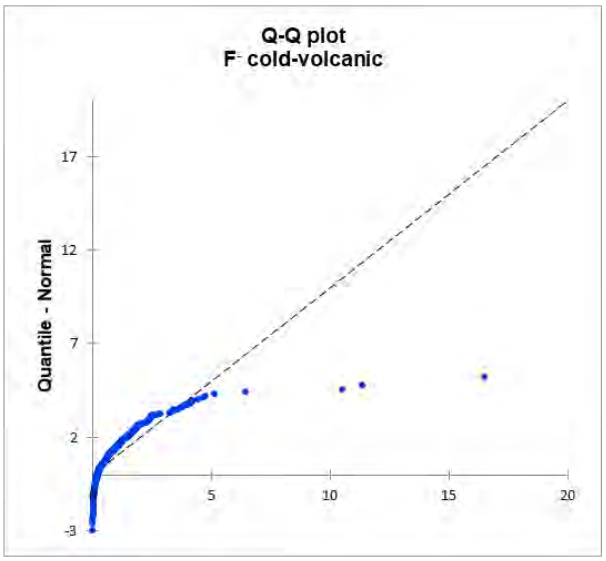
Q-Q plot
F- cold-volcanic
Quantile - Normal
17
12
7
2
-3
5
10
15
20

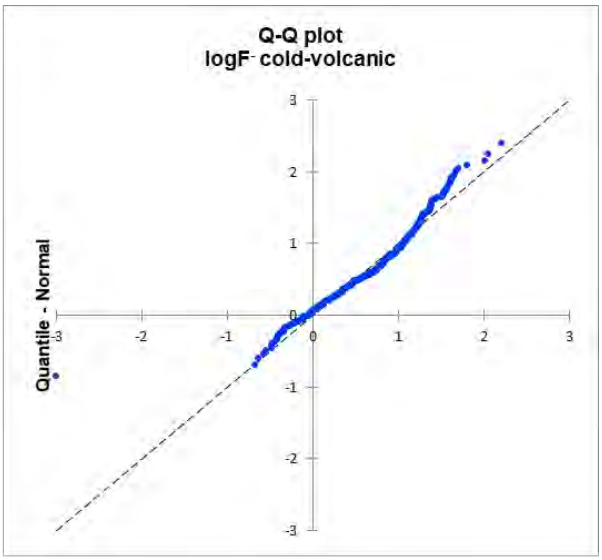
Q-Q plot
logF- cold-volcanic
Quantile - Normal
3
2
1
0
-1
-2
-3
-3
-2
-1
0
1
2
3

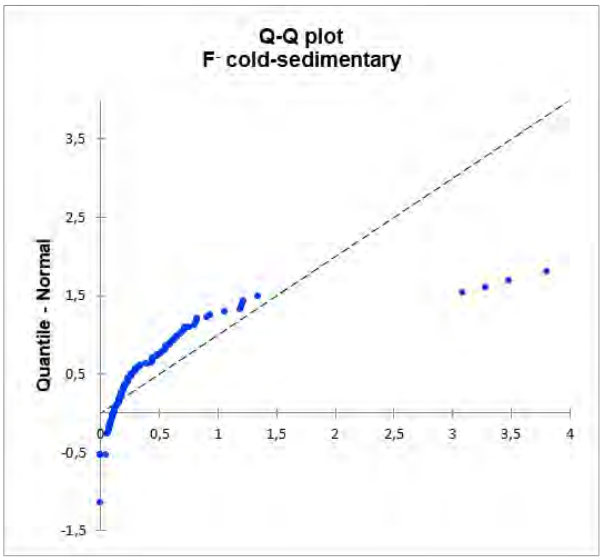
Q-Q plot
F- cold-sedimentary
Quantile - Normal
3,5
2,5
1,5
0,5
-0,5
-1,5
0
0,5
1
1,5
2
2,5
3
3,5
4

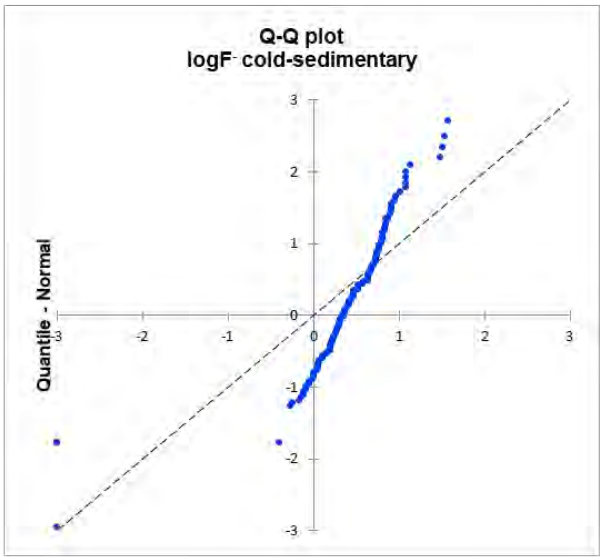
Q-Q plot
logF- cold-sedimentary
Quantile - Normal
3
2
1
0
-1
-2
-3
-3
-2
-1
0
1
2
3

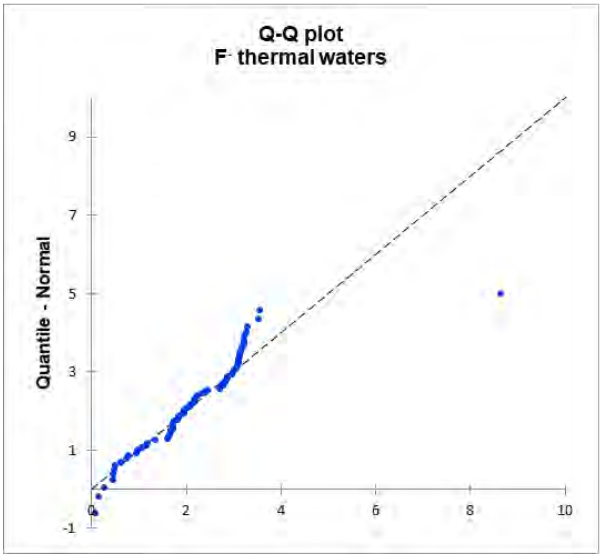
Q-Q plot
F- thermal waters
Quantile - Normal
9
7
5
3
1
-1
0
2
4
6
8
10

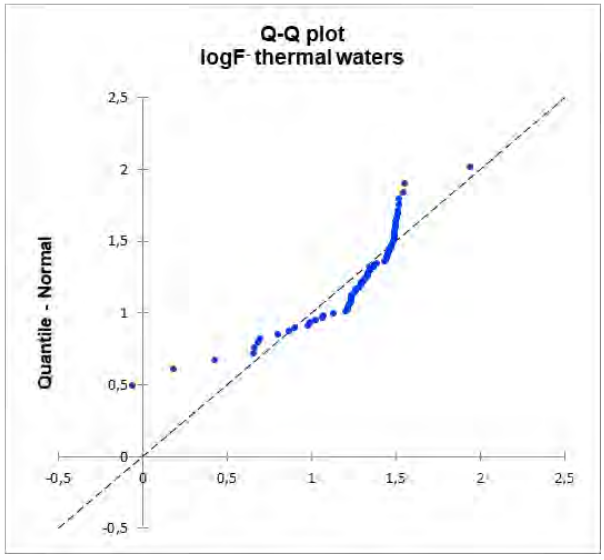
Q-Q plot
logF- thermal waters
Quantile - Normal
2,5
2
1,5
1
0,5
0
-0,5
-0,5
0
0,5
1
1,5
2
2,5

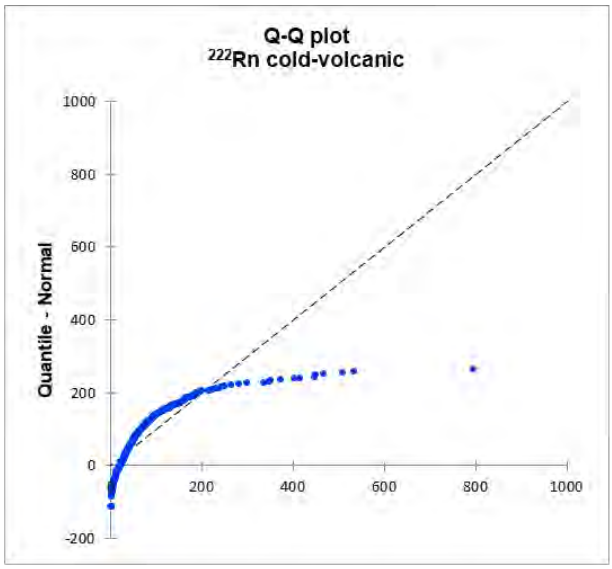
Q-Q plot
222Rn cold-volcanic
Quantile - Normal
1000
800
600
400
200
0
-200
200
400
600
800
1000

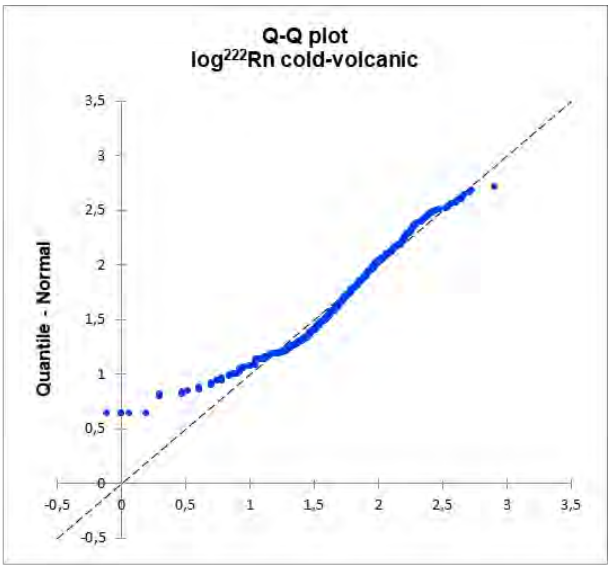
Q-Q plot
log222Rn cold-volcanic
Quantile - Normal
3,5
3
2,5
2
1,5
1
0,5
0
-0,5
-0,5
0
0,5
1
1,5
2
2,5
3
3,5

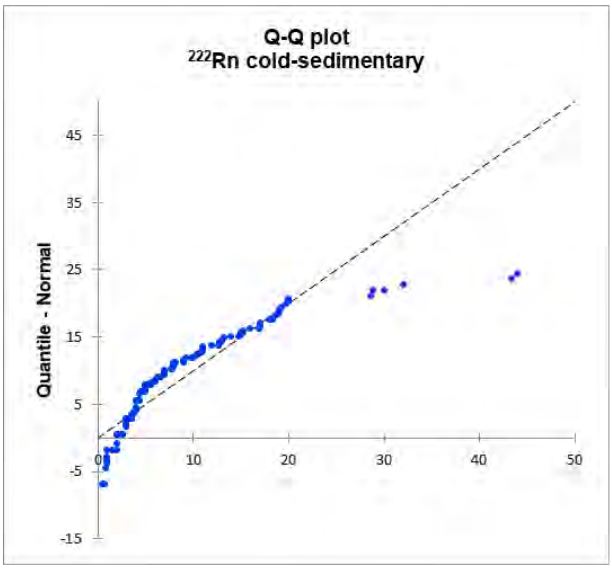
Q-Q plot
222Rn cold-sedimentary
Quantile - Normal
45
35
25
15
5
-5
-15
0
10
20
30
40
50

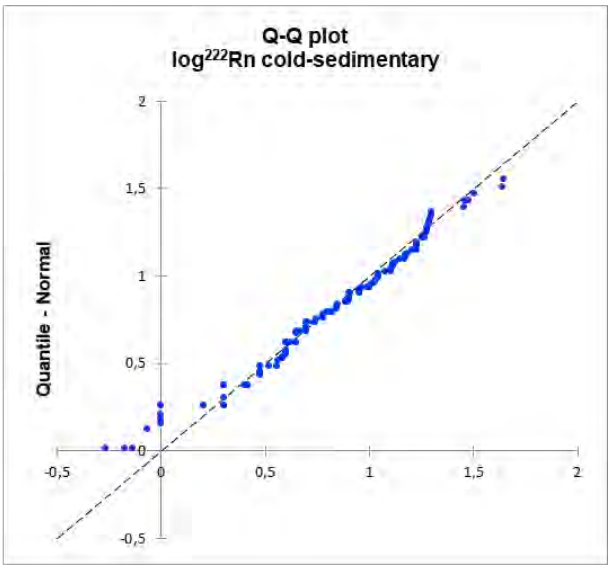
Q-Q plot
log222Rn cold-sedimentary
Quantile - Normal
2
1,5
1
0,5
0
-0,5
-0,5
0
0,5
1
1,5
2

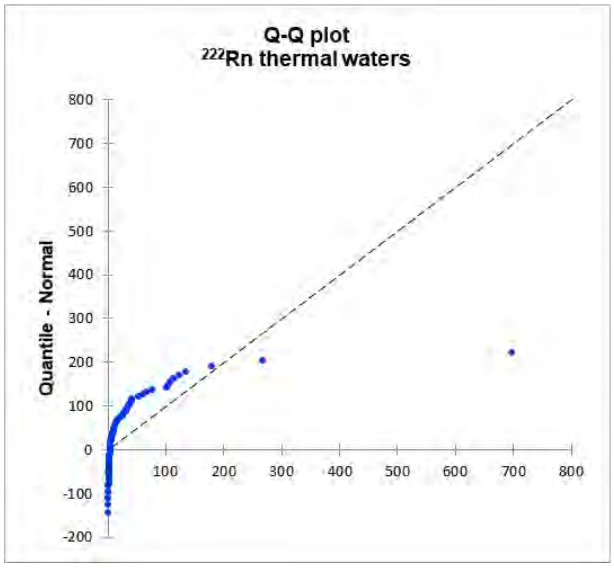
Q-Q plot
222Rn thermal waters
Quantile - Normal
800
700
600
500
400
300
200
100
0
-100
-200
100
200
300
400
500
600
700
800

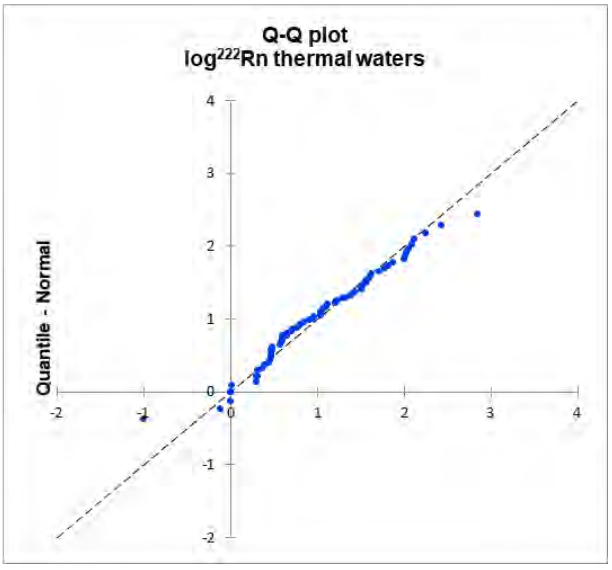
Q-Q plot
log222Rn thermal waters
Quantile - Normal
4
3
2
1
0
-1
-2
-2
-1
0
1
2
3
4

Supplementary Material 4

Semi-variogram parameters (ARSENIC)	**Structural model parameters**
Variable = log (As) Lag = 2000 m Number of lags = 12 Angular tolerance = 45° Maximum continuity direction (U) = N140°E Minimum continuity direction (V) = N230°E	Structure = Nugget + Spherical (2 sills) Nugget parameters: Sill (c_1) = 1.30 Spherical model parameters: Sill (c_2) = 1.50 Sill (c_3) = 0.55 Range U = 12000 m Range V = 11000 m
Cross-validation	**Neighborhood parameters**
Mean error = 0.82 Root-mean-square = 101.4 Mean standardized error = 0.014 Root-mean-square standardized = 1.007	Type = moving Major axis orientation = N140°E Minor axis orientation = N230°E Major axis measure = 12000 m Minor axis measure = 11000 m Number of sectors = 8 Minimum number of samples = 2 Optimum number of samples = 5

Semi-variogram parameters (FLUORIDE)	**Structural model parameters**
	Structure = Nugget + Spherical (2 sills)
Variable = log (F^-)	Nugget parameters:
Lag = 2500 m	Sill (c_1) = 1.20
Number of lags = 12	Spherical model parameters:
Angular tolerance = 45°	Sill (c_2) = 1.10
Maximum continuity direction (U) = N160°E	Sill (c_3) = 0.90
Minimum continuity direction (V) = N250°E	Range U = 9000 m
	Range V = 8500 m
Cross-validation	**Neighborhood parameters**
Mean error = 0.82	Type = moving
	Major axis orientation = N160°E
Root-mean-square = 1.72	Minor axis orientation = N250°E
	Major axis measure = 9000 m
Mean standardized error = -0.050	Minor axis measure = 8500 m
	Number of sectors = 8
Root-mean-square standardized = 2.667	Minimum number of samples = 2
	Optimum number of samples = 5

Semi-variogram parameters (RADON)	**Structural model parameters**
	Structure = Nugget + Spherical (2 sills)
Variable = log (^{222}Rn)	Nugget parameters:
Lag = 2500 m	Sill (c_1) = 0.75
Number of lags = 12	Spherical model parameters:
Angular tolerance = 45°	Sill (c_2) = 0.90
Maximum continuity direction (U) = N170°E	Sill (c_3) = 0.25
Minimum continuity direction (V) = N260°E	Range U = 8500 m
	Range V = 8000 m

Cross-validation	**Neighborhood parameters**
Mean error = 9.40	Type = moving
	Major axis orientation = N170°E
Root-mean-square = 81.09	Minor axis orientation = N260°E
	Major axis measure = 8500 m
Mean standardized error = -0.023	Minor axis measure = 8000 m
	Number of sectors = 8
Root-mean-square standardized = 0.923	Minimum number of samples = 2
	Optimum number of samples = 5